Environmental Modelling and Software 109 (2018) 114–133

Contents lists available at ScienceDirect

Environmental Modelling & Software

journal homepage: www.elsevier.com/locate/envsoft

Modelling hydrology and water quality in a mixed land use catchment and eutrophic lake: Effects of nutrient load reductions and climate change

Wang Me[a,b,*], David P. Hamilton[a,1], Christopher G. McBride[a], Jonathan M. Abell[c], Brendan J. Hicks[a]

[a] Environmental Research Institute, University of Waikato, Private Bag 3105, Hamilton, 3240, New Zealand
[b] College of Hydrology and Water Resources, Hohai University, Nanjing, 210098, People's Republic of China
[c] Ecofish Research Ltd., Suite 1220–1175 Douglas Street, Victoria, British Columbia, Canada

ARTICLE INFO

Keywords:
Catchment modelling
Lake modelling
Nutrient reductions
Climate change
Lake eutrophication

ABSTRACT

The objective of this study was to combine a catchment model with a one–dimensional lake water quality model to simulate the trophic state of a eutrophic shallow lake in response to nutrient load reductions and climate change. The catchment and lake models gave satisfactory performance in simulating observed data, indicating that the key processes that affect nutrient loads and lake trophic status were adequately represented. Simulating removal of nutrients by reducing fertiliser applied to farmland or irrigated wastewater had minor effects on nutrient concentrations in the lake, but simulations using a projected climate for 2090 showed a major impact on nutrients and water quality. This overarching effect indicated that polymictic lakes may be particularly vulnerable to eutrophication associated with climate change due to increased internal nutrient loading, which will lead to a biological response of increased algal biomass, while changes in external loads will have lesser relative impact.

Software

The catchment modelling used Soil and Water Assessment Tool (SWAT2012 rev629; released in July 2014) developed by Dr Jeff Arnold (the United States Department of Agriculture, Agricultural Research Service) and available as open–source software in FORTRAN language (http://swat.tamu.edu/). The lake water quality modelling used DYnamic REservoir Simulation Model – Computational Aquatic Ecosystem DYnamics Model (DYRESM–CAEDYM, version 4.0; released in 2012) originally developed at the Centre for Water Research, the University of Western Australia and written in FORTRAN language. Software from the Centre for Water Research is maintained by Hydronumerics (http://hydronumerics.com.au/).

1. Introduction

Increased nutrient loads from agricultural and municipal wastewater sources have dramatically reduced the ecological quality of receiving waterbodies in many lake catchments (Foote et al., 2015; Hussain et al., 2002). In many catchments, actions are underway to address point and diffuse sources of nutrient pollution, as mandated by environmental regulation and community concerns regarding water quality (Scavia et al., 2014; Hamilton et al., 2016). Examples of such actions include the diversion of wastewater discharges (OECD, 2001; Krebs, 2008), changes to farming practices and agricultural land use (Abell et al., 2011), or the use of a range of geo–engineering techniques (e.g., Spears et al., 2013), including the application of alum (aluminium sulphate) to lake inflows (Smith et al., 2016).

In addition to the management changes described above, changes in climate are predicted to affect the hydrological cycle and thus also modify nutrient transformation and transport processes in terrestrial and aquatic environments. For example, an increase in total phosphorus (TP) loads of 3.3%–16.5% in Danish streams in the next century was predicted by Jeppesen et al. (2009), mostly in response to increased precipitation in winter. A climate–induced increase in the loss of total nitrogen (TN) from a small Mediterranean catchment (30 km^2) in Slovenia was predicted by Glavan et al. (2015), who applied six climate scenarios for three future periods (2030s, 2060s, 2090s). Their modelled changes in TN loads (2061–2090) ranged from 5.3% to 80.2%, mostly in response to increasing precipitation. On the contrary, other studies have indicated that nutrient loading for the catchment may actually go down with climate warming primarily because warmer air

* Corresponding author. Environmental Research Institute, University of Waikato, Private Bag 3105, Hamilton, 3240, New Zealand.
E-mail address: yaowang0418@gmail.com (W. Me).
[1] Present address: Australian Rivers Institute, 170 Kessels Road, Nathan, Qld, 4111, Australia.

https://doi.org/10.1016/j.envsoft.2018.08.001
Received 7 December 2017; Received in revised form 1 August 2018; Accepted 1 August 2018
Available online 13 August 2018
1364-8152/

temperatures increase evaporation, resulting in less runoff. Robertson et al. (2016) projected decreases in total annual streamflow (−1.8% average, ranging from −21.2% to +8.9%) and TP loads (−3.1% average, ranging from −21.2% to +8.9%) for the Lake Michigan Basin by 2045–2065, in consideration of the projected variability in total annual precipitation (+5.1% average, ranging from −5.1% to +16.7%) and average annual air temperature (+2.6 °C average, ranging from +2.1 to +4.0 °C).

Climate change also directly influences lake water temperature and stratification, which may in turn modify in–lake nutrient dynamics (Arnell et al., 2015). A modelling study of three New Zealand lakes (Trolle et al., 2011) showed that the effect on water quality of a mid–range climate warming projection for 2100 would equate to increasing external nutrient loads by 25–50%. Similarly, Hamilton et al. (2012) showed negative effects of future climate on lake water quality, including increased trophic state and frequency of cyanobacteria blooms. Climate change could also affect the transport and processing of nutrients in lake catchments, as well as processes within receiving waters. Some of these processes may be synergistic whereby increased catchment nutrient loads interact with higher water temperatures to stimulate growth of bloom–forming cyanobacteria (Hamilton et al., 2016).

Few studies have connected climate, catchment and lake models to provide ecosystem–scale assessments of hydrological and water quality responses to climate change and changes in catchment nutrient loads. General circulation models (GCMs), downscaled by pattern scaling methods (Santer et al., 1990) provide future climate scenarios at a regional scale (Tebaldi and Arblaster, 2014; Herger et al., 2015) and have been applied to examine impacts on freshwater resources (Todd et al., 2011) and terrestrial processes (Huntingford et al., 2010). The main assumption underlying the pattern scaling method is that the local response of a climate variable is linearly related to the global mean temperature change (Mitchell, 2003). This theory has some limitations in projecting future extreme events (Lustenberger et al., 2014) and the spatial variability of climate data (Tebaldi and Arblaster, 2014). To overcome these limitations, ensemble simulations using multiple GCMs are recommended for the assessment of climate change impacts (Murphy et al., 2007; Lopez et al., 2014).

To assess temporal responses of receiving environments to catchment inputs, studies have been undertaken that link outputs from a catchment model (e.g., SWAT: Soil Water and Assessment Tool) to a water quality model (e.g., CE–QUAL–W2, Debele et al., 2008; WASP, Narasimhan et al., 2010, or; DYRESM–CAEDYM, Copetti et al., 2006). The process–based catchment model SWAT provides the ability to simulate time–varying land management practices in catchments (Neitsch et al., 2011), and has been applied to a small number of New Zealand catchments (e.g., Cao et al., 2006; Morcom, 2013; Me et al., 2015). DYRESM–CAEDYM, a process–based, one–dimensional hydrodynamic–biogeochemical aquatic ecosystem model, can be used to simulate in–lake processing of nutrients and biological responses (Hamilton and Schladow, 1997). It has been applied to lakes across the globe (Bruce et al., 2006; Trolle et al., 2008) and to several New Zealand lakes to predict water quality and trophic state (Rutherford et al., 1996; Burger et al., 2008; Trolle et al., 2011). DYRESM–CAEDYM has been supplied with inflow data from simulations using the SWAT model for a catchment in North Italy (Copetti et al., 2006) to examine seasonal trends in lake surface water temperature, water column thermal gradients and dynamics of phosphorus and phytoplankton.

Lake Rotorua, located in the Bay of Plenty Region of the North Island of New Zealand, is a nationally–iconic water body and plays a significant role in recreation and tourism at national scale. However, eutrophication has increased due to intensification of catchment land use (Hamilton et al., 2012). The original dominant land cover of Lake Rotorua catchment was indigenous forest but has been replaced by pastoral land since the first European settlement in the 1880s (Mueller et al., 2015). By 1978, pastoral land had become the dominant land cover (52.9%) in the Lake Rotorua catchment, followed by indigenous forest (30.6%) and exotic forest (8.3%; Environment Bay of Plenty, 1997). Land cover in the Lake Rotorua catchment remained relatively stable from 1978 to 1996, with only 1% of pastoral land and 5.5% of indigenous forest converted into exotic forest (Environment Bay of Plenty, 1997). The dominant soil types in the Lake Rotorua catchment are volcanic and pumice soils with low clay contents and low bulk density (Environment Bay of Plenty, 2010). Approximately 43% of land in the catchment has a slope of 0 to 8° but there are steeper areas of land (15%) in the outer catchment of slope > 26°. There is a gradient of rainfall from 1.2 m y^{-1} in the east and near the lake to 2.5 m y^{-1} in the hilly western area of the catchment (available at http://www.rotorualakes.co.nz/rotorua). Urban wastewater was discharged to Lake Rotorua until 1991 after which time forest blocks in one lake sub–catchment (Puarenga) have been irrigated with treated municipal wastewater. Resource consent conditions for wastewater disposal to the forest blocks restrict TN and TP wastewater losses to the receiving stream to 30 t yr^{-1} and 3 t yr^{-1}, respectively. Previous assessments of nutrient losses have indicated some non–compliance with the TN consent limit and there is some indication of an increase in TP loading to the receiving stream since 2002 (Me et al., 2017). These increases may be caused by a number of factors including the application rate of wastewater, increases in the nutrient load from non–irrigated areas within the catchment, forest operations not associated with wastewater irrigation and altered rainfall patterns. The Puarenga Stream sub–catchment is also representative of typical land cover, soil type and slope of the entire Lake Rotorua catchment and the Puarenga Stream contributes ~16% of total nutrient loads to Lake Rotorua (Abell et al., 2015). The SWAT2012 model was used in this study to simulate discharge and nutrient loads from the Puarenga Stream (the second largest surface inflow to Lake Rotorua) under current land use practices (including treated wastewater irrigation) and climate, to provide a "reference" condition. The model was only set up for the Puarenga Stream catchment because the information required for model setup for other lake sub–catchments was limited and one of the major objectives was to examine the effects of treated wastewater irrigation (specific to the Puarenga Stream) on lake water quality and to assess how a suite of scenarios of nutrient reductions and climate change might affect nutrient loads in the Puarenga Stream (using SWAT2012 rev629) and water quality in Lake Rotorua (using DYRESM–CAEDYM version 4.0). Coupling of these two models (i.e., output from SWAT2012 as input for DYRESM–CAEDYM to simulate common variables) was used in this study to better understand the potential for synergistic or antagonistic interactions between regional climate change and nutrient load reductions in the Puarenga Stream catchment to influence water quality in Lake Rotorua.

2. Material and methods

2.1. Study area and measured data

Lake Rotorua is located in the North Island of New Zealand (Fig. 1) and has a warm temperate climate. Annual mean precipitation (at 280 m asl) is 1252 mm, air temperature 12.6 °C, relative humidity 81%, short–wave radiation 170 W m^{-2}, and wind speed 3.6 m s^{-1} (at 10 m above the water surface) based on the period July 2006–June 2010. The predominant wind directions are south–west and north–east. Annual mean values of the aforementioned meteorological variables were derived from records at Kaituna rain gauge and Rotorua Airport Automatic Weather Station (Fig. 1; National Climatic Database; available at http://cliflo.niwa.co.nz/).

Lake Rotorua (surface area 80.8 km^2, mean depth 10.8 m) is a polymictic, temperate lake which receives inflow from nine major surface streams and nine smaller surface streams (Fig. 1; Hoare, 1980). The only surface outflow (mean annual discharge 18.5 m^3 s^{-1}) is the Ōhau Channel (Fig. 1; Hoare, 1980). The residence time of Lake

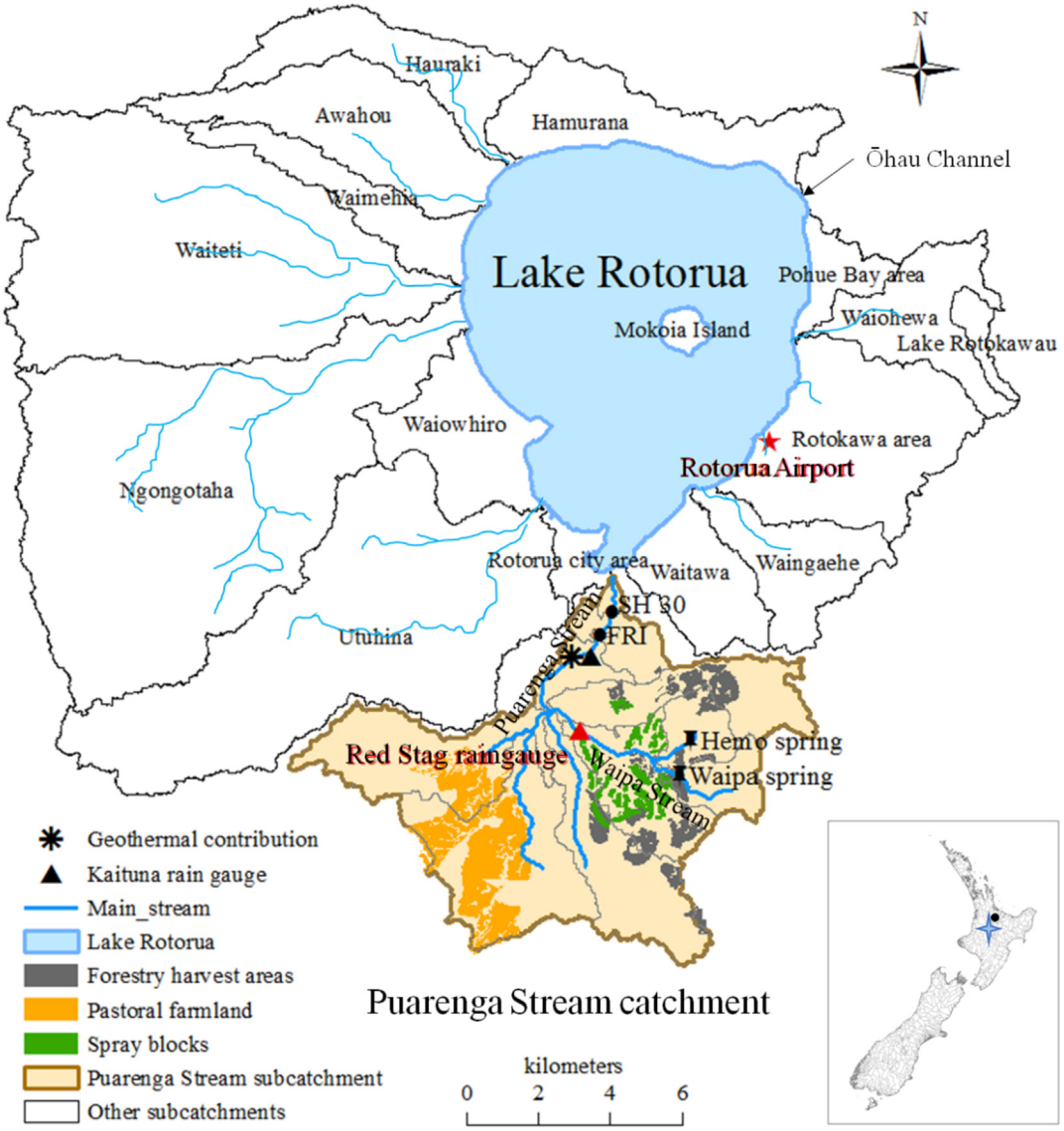

Fig. 1. Lake Rotorua surface topographic catchment showing the major sub–catchments with the major streams. The Puarenga Stream catchment modelled in this study is located in the south. Managed land areas are shown within the Puarenga Stream catchment for which management schedules were prescribed in the SWAT2012 model. Water samples were collected at the Forest Research Institute (FRI) stream–gauge, which was repositioned in June 2010 to State Highway 30 (SH 30). The only outlet from Lake Rotorua is the Ōhau Channel. Inset: Map of New Zealand showing location of Rotorua.

Rotorua is 1.5 years. Surface water temperature at 0.5 m in Lake Rotorua ranges from 10 °C to 22 °C for 2006–2010 (Abell et al., 2015). The regional management authority, Bay of Plenty Regional Council (BoPRC), has assigned a target Trophic Level Index (TLI) for Lake Rotorua of 4.2. The TLI is commonly used in New Zealand to quantify trophic state and integrates annual mean values of four variables: Secchi disc depth (a measure of transparency) and concentrations of Chl *a*, TP, and TN (Burns et al., 1999). The target value of 4.2 for Lake Rotorua corresponds to a eutrophic status (i.e., between 4 and 5) and is based on historical data for around 1970, when the lake was deemed to have acceptable water quality (Scholes, 2011). Alum dosing of two inflows has been used to reduce TP in Lake Rotorua and, correspondingly, the TLI (Smith et al., 2016). The first dosing station commenced operation in the Utuhina Stream in June 2006 and the second dosing commenced in the Puarenga Stream in January 2010 (Fig. 1). The sampling site for the Utuhina Stream is downstream of the dosing station and therefore the effects of alum dosing are implicit in the monitoring data of the Utuhina Stream (i.e., the measured concentrations of dissolved reactive phosphorus reflect the reductions caused by alum dosing upstream, which first commenced in the Utuhina Stream in June 2006). A second dosing plant was implemented in the Puarenga Stream in January 2010, with the sampling site for the Puarenga Stream upstream of the dosing station. Measured data for Lake Rotorua during January 2008–June 2010 were used for DYRESM–CAEDYM baseline simulations. Therefore, concentrations of dissolved reactive phosphorus in the Puarenga Stream would not have reflected alum effects in the lake model for the period from January 2010 to June 2010 but likely had minimal impact on simulation output. Water temperatures and concentrations of phosphate (PO_4–P), ammonium–nitrogen (NH_4–N), nitrate–nitrogen (NO_3–N), TP, TN, dissolved oxygen (DO) and Chl *a* are monitored monthly at two depths (integrated 0–6 m and 19 m) in Lake Rotorua by BoPRC.

The Puarenga Stream is the second largest surface inflow to Lake Rotorua and drains a catchment of 77 km^2 (Fig. 1). The Puarenga Stream subcatchment catchment elevation is from 280 m asl where it enters Lake Rotorua, to 761 m asl. It is moderately steep (mean slope = 9% or 5.7°) and the predominant land uses are exotic *Pinus radiata* forest (47%) and pastoral farmland (26%; New Zealand Land

Cover Database Version 2). There are two substantive cold–water springs (Waipa Spring and Hemo Spring) and one geothermal spring within the catchment area (Fig. 1). Cold–water springs in the Puarenga catchment originate from aquifers in the underlying volcanic geology (Morgenstern et al., 2015) and contribute a high TP load (8.75 t P yr^{-1}) to the Puarenga Stream (Kim Lockie; Rotorua Lakes Council; personal communication). Fertiliser (~40 t yr^{-1} of P and 127 t yr^{-1} of N) has been applied to 8 km^2 of pastoral farmland (Fig. 1) in the Puarenga Stream catchment since about 1950 (Anastasiadis et al., 2011). Urea is typically applied twice, in winter and spring, and four times during summer and autumn, at a total rate of ~200 kg ha^{-1} yr^{-1} of N; di–ammonium phosphate is applied once or twice, in spring and autumn, at a total rate equivalent to ~50 kg ha^{-1} yr^{-1} of P (Alastair McCormick; BoPRC; personal communication). Treated municipal wastewater has been applied to up to 16 forestry blocks in the Whakarewarewa Forest (~2 km^2 in total; Fig. 1) since 1991, at a rate of ~19,000 m^3 d^{-1}, which equates to approximately 25 t yr^{-1} of P and 53 t yr^{-1} of N. The initial irrigation schedule involved applying wastewater to two blocks with a daily rotation (i.e., a total of 14 blocks were irrigated weekly). Since 2002, wastewater has been irrigated daily on 10–14 blocks (Lowe et al., 2007). The irrigated land treatment area has allophanic soils which retain 85–95% of the irrigated P (Beets et al., 2013), and the unirrigated area has mostly pumice soils that have moderate (50–60%) soil sorption capacity for P (Saunders, 1965; Fertiliser & Lime Research Centre, 2014).

Puarenga Stream water samples were collected at the Forest Research Institute (FRI) stream–gauge (1.7 km upstream of Lake Rotorua; Fig. 1) by BoPRC. Measurements at the FRI stream–gauge were considered representative of the contribution of the Puarenga Stream catchment to Lake Rotorua. Discharge data were collected by BoPRC at 15-min intervals for the period 2005 through 2010 (annual mean 2.2 m^3 s^{-1}). Discharge records of the Puarenga Stream during 1998–2004 were intermittent because the FRI stream–gauge was closed in mid–1997 and reopened late in 2004 (Environment Bay of Plenty, 2007). Measured data for the Puarenga Stream before June 2010 were used for the SWAT2012 model baseline simulation as the FRI stream–gauge was thereafter repositioned 720 m downstream to State Highway 30 (SH 30) (Fig. 1). Concentrations of suspended sediment (SS), dissolved reactive phosphorus (DRP), organic phosphorus (ORGP), NH_4–N, NO_3–N, organic nitrogen (ORGN), TP and TN were measured monthly in the Puarenga Stream (Scholes, 2011). Daily surface inflow and nutrient concentrations of eight other major inflows of Lake Rotorua were measured and nine minor inflows were estimated by Abell et al. (2015; see Table 1) for the same period as the Puarenga Stream. Based on these data, the Puarenga Stream contributes 16.5% of total inflow volume, 15.6% of TP load, and 16.2% of TN load to Lake Rotorua (Table 1). The locations of contributing catchments are shown in Fig. 1.

2.2. Model configuration

Key SWAT input data requirements included: a digital elevation model (DEM; elevation range 283–761 m; 25 m horizontal resolution) obtained from BoPRC; meteorological records from Rotorua Airport Weather Station; rainfall data from the Kaituna and Red Stag rain gauges; records of two cold–water springs and one geothermal spring, flow rates and nutrient concentrations in spring discharges which were configured as point sources; a stream digital map obtained from BoPRC; soil characteristics (e.g., the soil profile can be divided into ten layers in the SWAT model; Arnold et al., 2013) obtained from S–map (developed by Landcare Research; see http://smap.landcareresearch.co.nz/home); land use classifications (obtained from New Zealand Land Cover Database Version 2 which relates to the year 2002); and management schedules (obtained from BoPRC) for key land uses (i.e., pasture fertilisation, wastewater irrigation and timber harvesting). The source of irrigation was specified in the model as outside of the catchment, reflecting that the treated wastewater was sourced from the wider area (e.g., rather than abstracted from surface water in the Puarenga sub–catchment). Daily wastewater irrigation was configured for each block by defining separate irrigation and fertilisation management schedules to define the input of water and nutrients, respectively, to the model. The required daily irrigation depths were based on daily irrigation volumes for each block. Nutrients in the irrigated wastewater were assigned a daily composition configured from monthly mean concentrations measured in 7–day composite samples of the irrigated–wastewater. Configuration of forest harvest operations was based on annual harvesting data provided by forestry managers. Each block was assumed to be mature at the start of the modelling period. Harvesting of each block was configured as a clear–fell operation that took one year to complete, during which time no irrigation was carried out (Alison Lowe, Rotorua Lakes Council, *pers. comm.*). Only one to three forested blocks were harvested at a time, consistent with records. The delineation of the Puarenga Stream catchment (Me et al., 2015) included ten sub–catchments (Fig. 1) and 622 hydrological response units (HRUs). The SWAT2012_rev629 code was used which includes modifications to hourly simulations of SS loads in–stream, nutrient applications in management practice, and some unit corrections in soil nutrient cycling calculations. Further details of code modifications are outlined in Me (2017).

The SWAT2012 model was not set up for eight other major catchments or nine minor catchments because the information required for model setup was limited and a key objective of the study was to examine the effects of treated wastewater irrigation (specific to the Puarenga Stream) on lake water quality. Instead, other inflow input data were configured using either measurements or values derived from Abell et al. (2015; see Table 1).

The DYRESM–CAEDYM model (version 4.0) was used to simulate hydrodynamic and biogeochemical processes in Lake Rotorua. Key forcing data were climate, bathymetry, inflow volume and nutrient

Table 1
Inflow catchments of Lake Rotorua. Six inflow catchments were classified as surface (S) water–dominated catchments and four as groundwater (G)–dominated catchments (see Subsection 2.2). Mean annual inflow water temperature (T_{inf}), discharge, concentrations of total phosphorus (TP) and total nitrogen (TN), and percentage of inflow volume, TP and TN load contributions were derived from Abell et al. (2015) for July 2006 to June 2010.

Catchment name	Water source	Catchment area (km^2)	T_{inf} (°C)	Discharge (m^3 s^{-1})	Inflow volume (%)	TP (mg L^{-1})	TP load (%)	TN (mg L^{-1})	TN load (%)
Awahou	G	19.9	15.4	1.9	14.3	0.065	14.6	1.38	17.3
Hamarana	G	16.0	12.4	2.6	19.6	0.077	23.7	0.77	13.2
Ngongotaha	S	77.4	11.0	2.0	15.0	0.043	10.2	0.98	12.9
Puarenga	S	77.0	14.5	2.2	16.5	0.060	15.6	1.12	16.2
Utuhina	S	61.0	12.8	1.8	13.5	0.057	12.1	0.95	11.3
Waingaehe	G	11.0	15.4	0.3	2.3	0.106	3.8	1.60	3.2
Waiohewa	S	11.7	13.4	0.4	3.0	0.067	3.2	2.56	6.8
Waiowhiro	S	13.6	12.7	0.3	2.3	0.057	2.0	0.95	1.9
Waiteti	G	61.9	11.8	1.4	10.5	0.052	8.6	1.41	13.0
Minor streams	S	61.1	16.0	0.4	3.0	0.130	6.2	1.61	4.2

concentrations, and outflow volume. The nine major inflows were classified into surface water–dominated or groundwater–dominated based on the variability of daily inflow water temperature. Catchments where mainstem water temperatures ranged > ± 25% of their multi–year daily mean water temperature were defined as surface water–-dominated and the remainder as groundwater–dominated (see Table 1). The remaining nine minor streams were represented as a single inflow representing the residual term of the lake water balance used in DYRESM–CAEDYM. A lake water balance to estimate additional residual inflow was calculated after the method described in Hamilton et al. (2012). The inflow from minor streams was assumed to be predominantly surface waters. Outflow via the Ōhau Channel represented in the lake model was based on daily mean discharge measurements provided by the National Institute of Water and Atmospheric Research (NIWA).

2.3. Model calibration and validation

Simulation results were generated at daily intervals from SWAT2012 for the four–hydrological–year baseline period from July 2006 to June 2010. The calibration period was July 2006 to June 2009, and the validation period was July 2009 to June 2010. This period coincided with when alum dosing started in June 2006 (Smith et al., 2016) and the stream gauge repositioning in July 2010. One year was used for the SWAT2012 model warm–up and its simulations from July 2006 were used to drive DYRESM–CAEDYM. The lake model warm–up was from June 2006 to December 2007, corresponding to the 1.5-year lake residence time and a transition period of water quality first responding to alum dosing. The calibration period for the DYRESM–CAEDYM model was January 2008 to June 2009, and the validation period was July 2009 to June 2010.

Initial values of state variables required for the setup of both models were based on observed monitoring data that were measured close to the start date of the simulation period. Parameter values for the lake model (DYRESM–CAEDYM) were based on previous applications of the model for Lake Rotorua with subsequent adjustments of parameters for nutrient release rates from the bottom sediment (Burger et al., 2008) and particulate organic matter size and density (to increase sedimentation rates) to account for the in–lake effects of alum dosing (Hamilton et al., 2012; Abell et al., 2015). Minor adjustments were made based on one–at–a–time (OAT) calibration (Morris, 1991) using the mean values of measurements collected at the two lake sampling sites (see Subsection 2.1). For the SWAT2012 model, values of those parameters representative of the catchment physical characteristics were derived from measurements or literature, while the remainders were assigned by manual calibration within literature–specified limits. The OAT routine was applied to examine parameter sensitivity and calibrate the parameter values within carefully selected ranges for each simulated variable (Q, SS, ORGP, DRP, ORGN, NH_4–N, and NO_3–N) based on measurements collected at the FRI stream–gauge (Fig. 1). One parameter set was used for the whole Puarenga Stream catchment for the SWAT2012 application.

Daily mean values of 15–min discharge measurements (see Subsection 2.1) were used to calibrate SWAT parameters to simulate daily mean discharge in the Puarenga Stream. Measured nutrient and SS concentrations from monthly samples were converted to loads based on total discharge volume on the corresponding day. The measured monthly loads were then used to calibrate parameters by comparing with the simulations of nutrient loads from SWAT2012 on that sampling day.

Daily mean simulated discharge and nutrient concentrations for Puarenga Stream were used to evaluate the catchment model performance and then provide inputs to the lake model (DYRESM–CAEDYM). Inflow volume and nutrient concentrations for eight other major inflows and nine minor inflows of Lake Rotorua used in DYRESM–CAEDYM were based on the measured or estimated hydrologic and water quality data in Abell et al. (2015). Daily simulated concentrations from DYRESM–CAEDYM were compared with monthly mean values measured in the lake on that sampling day, and then used to evaluate the lake model performance. A modified “TLI3” (a three–variable TLI that excludes Secchi depth) was compared with model output because Secchi depth is not explicitly estimated by DYRESM–CAEDYM. The TLI target of 4.2 for Lake Rotorua is equivalent to a TLI3 value of 4.32 (Hamilton et al., 2015).

For both the catchment model (SWAT2012) and lake model (DYRESM–CAEDYM), model outputs from the “warm–up” period were not further considered for model evaluation. Model goodness–of–fit between simulated outputs and observations was initially assessed graphically and then quantified using four commonly–used model evaluation statistics (Moriasi et al., 2007): Pearson product moment correlation coefficient (r), root mean square error (RMSE), mean absolute error (MAE), and percent bias (PBIAS) (Appendix 1).

2.4. Model scenarios

2.4.1. Nutrient applications

As mentioned in Subsection 2.1, the predominant land uses in the Puarenga Stream catchment are exotic forest (47%) and pastoral farmland (26%) where treated municipal wastewater and fertilizer have been applied, respectively. Nutrient inputs to the Puarenga Stream catchment from treated municipal wastewater irrigation (Irr) and fertiliser applied on pastoral land (Pas) were assigned separately in the SWAT2012 model. Four nutrient scenarios were compared: 1) the current (“reference”) scenario, with both nutrient sources (S1–Irr1Pas1), 2) pasture fertilisation only (S2–Irr0Pas1), 3) wastewater irrigation only (S3–Irr1Pas0), and 4) no nutrient applications (S4–Irr0Pas0). Nutrient loadings from other catchments remained unchanged, i.e., simulations of different nutrient application scenarios were only undertaken for the Puarenga Stream catchment. The effects of nutrient reduction scenarios (S2–S4) on loads from the Puarenga Stream catchment and the water quality of Lake Rotorua (both surface and bottom waters) were analysed by calculating the percentage change relative to the reference scenario (S1) simulation.

2.4.2. Future climate projection

Future climate projections were determined with SimCLIM, a software package used for generating regional scenarios of future climate (Yin et al., 2013). The scenarios are based on the Intergovernmental Panel on Climate Change Fifth Assessment report (IPCC, 2013). The RCP8.5 scenario was chosen because it is representative of the pathway with the highest greenhouse gas emissions as a result of a higher increasing trend of population growth and a lower rate of technology development (Van Vuuren et al., 2011). This therefore provides for a precautionary approach when predicting environmental impacts. The RCP8.5 scenario corresponds to climate change equivalent to a short–wave radiation increase of 8.5 $W m^{-2}$ in 2100 due to increased levels of anthropogenic greenhouse gas emissions (Van Vuuren et al., 2011). Amongst the 40 GCMs presented in SimCLIM, 22 simulate all of the climate variables (Yin et al., 2013) required as input by SWAT and DYRESM–CAEDYM (Appendix 2).

A pattern scaling method (Santer et al., 1990) in SimCLIM produces regional change factors that were used in this study according to the SimCLIM 2013 Data Manual (Yin et al., 2013). Climate change perturbations were downscaled to regional scale using linear functions of the global annual mean temperature change using a method described in Mitchell (2003). Monthly median change factors (Touma et al., 2015) derived from the downscaled climate projections (Fig. 2) were used in the present climate data by adding to air temperature or by applying as a multiplicative factor to the other climate variables. Future changes in wind speed were not considered in this study because there is high uncertainty about relative change based on GCMs.

The current climate (hereafter CC0) was represented by the period

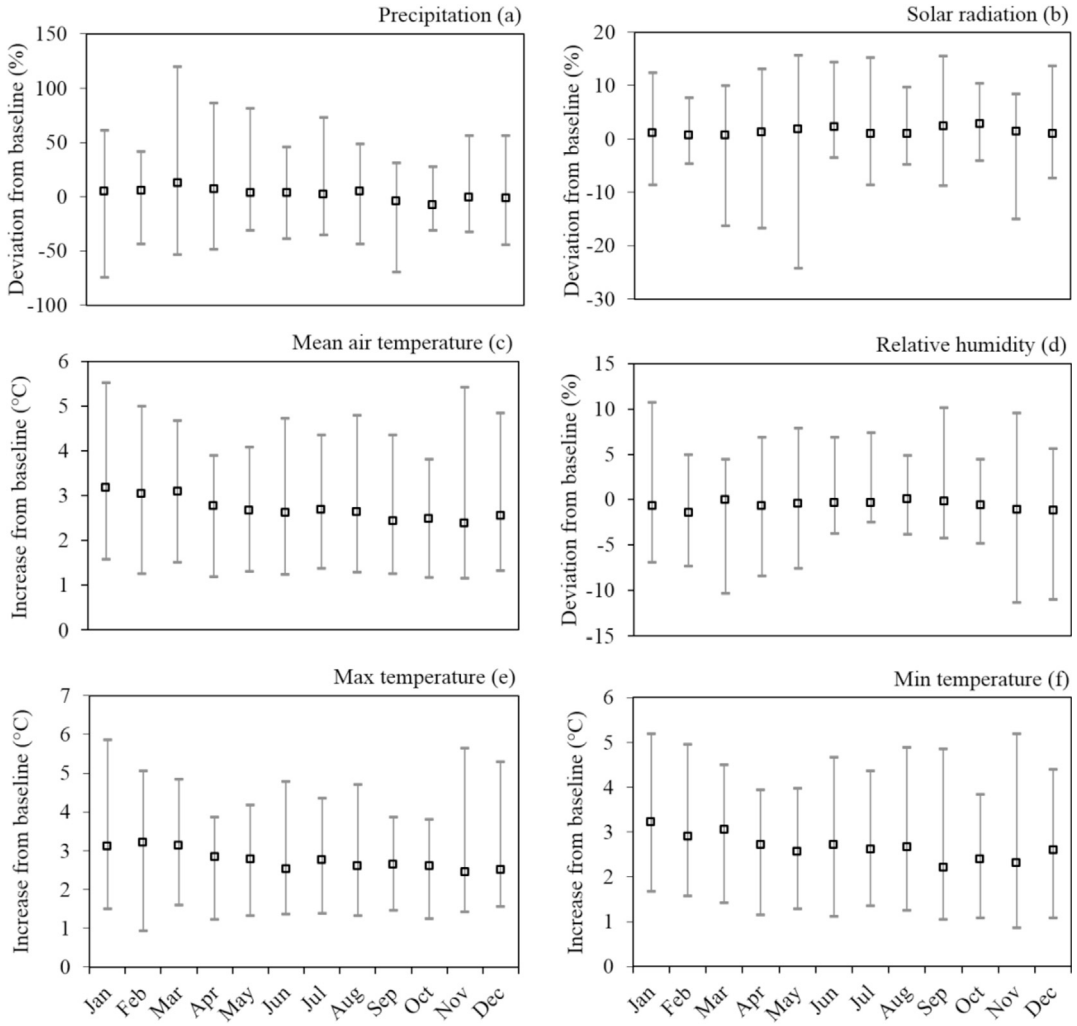

Fig. 2. Monthly median change factors (square markers) applied in 22 general circulation models (GCMs) that were used to generate 2090 regional climate data for modelling the Puarenga Stream catchment and Lake Rotorua. (a) precipitation; (b) solar radiation; (c) mean air temperature; (d) relative humidity; (e) maximum temperature; and (f) minimum temperature. Error bars indicate the range of monthly changes derived from the 22 GCMs.

from July 2005 to June 2010. SWAT baseline simulations used a subset of this period from July 2006 to June 2010 and DYRESM–CAEDYM used January 2008 to June 2010. Regional projections of global mean temperature change were derived for the period 2090–2099. The projected future climate of 2090 shows that precipitation will be higher from January to August (mid–summer to late winter) and lower from September to December (early spring to early summer), with annual mean air temperature increases of 2.7 °C (see Fig. 2).

The 2090 climate data, represented by adding direct addition to baseline air temperature or applying a multiplicative factor to baselines of other climate variables, were input to the SWAT2012 model to predict future (hereafter CC1) nutrient loadings from the Puarenga Stream catchment under the four scenarios of nutrient application (S1–S4). The future 2090 climate responses of Puarenga Stream to the lake examined the changes relative to reference scenario S1–Irr1Pas1 simulations. Monthly changes relative to scenario S2–Irr0Pas1 (with no wastewater irrigation) simulations were applied to the observed loads in other streams for consideration of the future climate impact on the lake (hereafter CC2). Climate change interactions with S2–Irr0Pas1 were considered because 1) other streams catchments did not have treated wastewater application; and 2) the Rotorua District Council has made a decision to cease irrigation to the Whakarewarewa Forest by 2019. For surface water–dominated catchments (see Subsection 2.2), the temperatures of major stream inflows were increased based on the increases predicted for the Puarenga Stream. For groundwater–dominated catchments, stream water temperatures were increased by adding 88% of the projected increase in air temperature, based on Kurylyk et al. (2013).

3. Results

3.1. Calibration and model performance

3.1.1. SWAT2012 model of the Puarenga Stream catchment

Optimised parameter values for the SWAT2012 model are presented in Appendix 3 for the whole Puarenga Stream catchment. Differences in some parameter values from previous SWAT2009 model runs in Me et al. (2015) reflected the modified SWAT2012 source code used in this study. Three parameter values were adjusted beyond the SWAT default range (Appendix 3): (1) the number of days for groundwater delay (GW_DELAY), (2) the phosphorus percolation coefficient (PPERCO), and (3) benthic (sediment) release rate for NH_4–N in the stream reach at 20 °C (RS3).

The parameter GW_DELAY (groundwater delay days) was set to 1825 days (five years) for the Waipa Stream sub–catchment, which was the value of mean groundwater residence time reported in Rutherford et al. (2009). This value was set as five years because in–stream nitrate concentrations appeared to reach a new equilibrium five–years after

treated wastewater was spray–irrigated within the Waipa Stream sub–catchment in 1991, which would be consistent with nitrate transport times in shallow groundwater (Rutherford et al., 2009). Recently, Morgenstern et al. (2015) re–examined the mean groundwater residence times for the wider Puarenga Stream catchment, which has a more complex groundwater system, and reported a mean value of c. 40 years.

The parameter PPERCO (phosphorus percolation coefficient) was adjusted because the Puarenga Stream catchment outside of the irrigation area has pumice soils with moderate P adsorption capacity (50–60%) and the wastewater spray blocks drained by the Waipa Stream have allophanic soil with high P adsorption capacity (85–95%) (see Subsection 2.1). The parameter value for RS3 (sediment release rate for in–stream NH_4–N, 50 mg m^{-2} d^{-1}) was based on Gabriele et al. (2013) who investigated headwater streams from an Austrian catchment where there is intensive agriculture and the stream channel is rich in organic material. Gabriele et al. (2013) estimated RS3 in the range 24–48 mg m^{-2} d^{-1}, so our value reflected high NH_4–N inputs and may have been reflective of some geothermal source inputs to the Puarenga Stream.

Simulations of discharge from the Puarenga Stream catchment showed high correspondence with measured values (Fig. 3a). Discharge peaks during high rainfall events were reasonably well simulated by the SWAT2012 model, although a few peaks were underestimated. Discharge after high rainfall events was overestimated, in particular during winter. Overall, the SWAT2012 model overestimated discharge by 3.9% during calibration (July 2006–June 2009) and 14.4% during validation (July 2009–June 2010) but with high values of r (> 0.8, $p < 0.001$; Table 2).

The range of concentrations of SS simulated by SWAT2012 was smaller than that of measured data from the Puarenga Stream catchment (Fig. 3b). Simulated and measured SS concentrations were positively correlated during calibration ($r = 0.45$, $p < 0.05$) but negative during validation ($r = -0.23$, $p > 0.05$; Table 2). Base flow SS concentrations were generally overestimated, and several peaks of SS concentrations were underestimated, contributing to an underestimate of SS concentrations of 4.3% during calibration and an overestimate of 5.3% during validation. The correlations between simulated and measured SS load were positive during calibration ($r = 0.52$, $p < 0.01$) and validation ($r = 0.30$, $p > 0.05$), with an underestimate of 3.9% during calibration and an overestimate of 17.2% during validation (Table 2).

Concentrations of P species were generally not simulated accurately for the Puarenga Stream catchment (Fig. 3c–e). The correlations were weak for both ORGP and DRP during calibration ($r \leq 0.25$, $p > 0.05$; Table 2) but were stronger during validation ($r = 0.70$, $p < 0.05$ for ORGP; $r = 0.68$, $p < 0.05$ for DRP). Concentrations of ORGP were overestimated by 27.9% and concentrations of DRP were underestimated by 9.8% during calibration, while during validation ORGP concentrations were underestimated by 23% and DRP concentrations were overestimated by 37.2% (Table 2). Concentrations of TP were overestimated by 11.3% during calibration and 0.3% during validation, with poor correlation statistics ($r = 0.05$, $p > 0.05$ for calibration; $r = 0.17$, $p > 0.05$ for validation; Table 2). However, simulated and measured ORGP and TP loads were positively correlated during calibration ($r = 0.48$, $p < 0.05$ for ORGP; $r = 0.59$, $p < 0.001$ for TP) and validation ($r = 0.89$, $p < 0.001$ for both; Table 2), reflecting the major impact of discharge on loads. Correlations between simulated and measured DRP loads were weak during calibration ($r = 0.12$, $p > 0.05$) and validation ($r = 0.22$, $p > 0.05$; Table 2).

The simulated concentrations of N species from the Puarenga Stream catchment showed high seasonal variability (Fig. 3f–i), with concentrations typically higher during the drier periods of summer and autumn, and lower during the wetter periods of winter and spring. Simulations of ORGN concentrations were generally within the range of measured data (Fig. 3f), although several measured peaks were underestimated during calibration (PBIAS = 0.5%), while base flow concentrations were overestimated during validation (PBIAS = −19.8%; Table 2). The correlations between simulated and measured ORGN concentrations were positive during calibration ($r = 0.47$, $p < 0.05$) and validation ($r = 0.75$, $p < 0.01$; Table 2). By contrast, correlations between simulated and measured NH_4–N concentrations were negative, with underestimates of 12.8% during calibration ($r = -0.47$, $p < 0.05$) and 15% during validation ($r = -0.31$, $p > 0.05$; Table 2). Simulations of NO_3–N and TN concentrations were strongly correlated with measurements during calibration ($r \geq 0.40$, $p < 0.05$) and validation ($r \geq 0.67$, $p < 0.05$), although NO_3–N and TN concentrations were underestimated by ~10% (see PBIAS in Table 2). Catchment loads of NO_3–N and TN were generally underestimated during

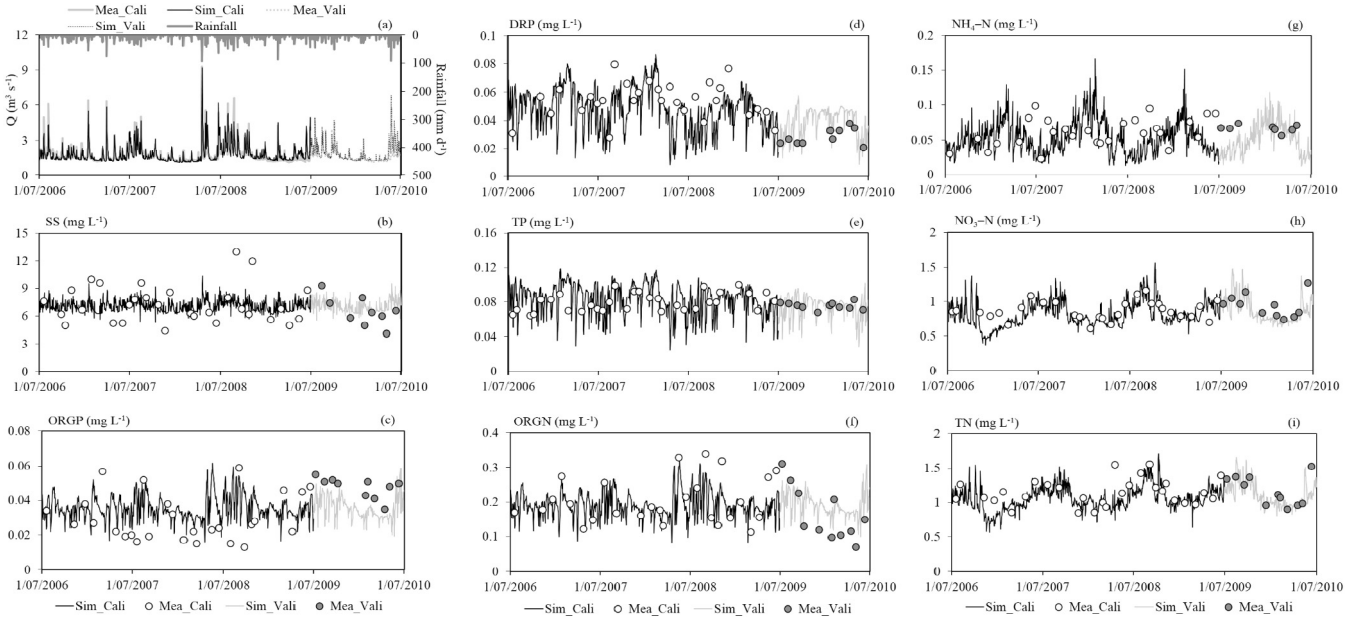

Fig. 3. Comparison of measurements taken at the FRI stream–gauge and SWAT2012 model outputs of (a) discharge (Q), concentrations of (b) suspended sediment (SS), (c) organic phosphorus (ORGP), (d) dissolved reactive phosphorus (DRP), (e) total phosphorus (TP), (f) organic nitrogen (ORGN), (g) ammonium–nitrogen (NH_4–N), (h) nitrate–nitrogen (NO_3–N) and (i) total nitrogen (TN) during calibration (July 2006 to June 2009) and validation (July 2009 to June 2010) periods.

Table 2
Statistical values of Pearson product moment correlation coefficient (r), root mean square error (RMSE), mean absolute error (MAE), and percent bias (PBIAS), used to assess SWAT2012 model performance for daily mean simulations of discharge (Q), loads and concentrations of suspended sediment (SS), organic phosphorus (ORGP), dissolved reactive phosphorus (DRP), total phosphorus (TP), organic nitrogen (ORGN), ammonium–nitrogen (NH_4–N), nitrate–nitrogen (NO_3–N) and total nitrogen (TN) from the Puarenga Stream catchment. Daily simulated discharge was compared with 15–min stream discharge data aggregated as daily mean values. Daily simulated concentrations were compared with monthly mean values measured on that sampling day. The significance of correlations between simulations and measurements was quantified based on the p value (see Subsection 2.2). $^{*}p < 0.05$; $^{**}p < 0.01$; $^{***}p < 0.001$. Units are relevant to RMSE and MAE values only.

Modelling period	Statistics	Q	SS	ORGP	DRP	TP	ORGN	NH_4–N	NO_3–N	TN
Calibration (July 2006–June 2009)		($m^3\ s^{-1}$)	Concentration ($mg\ L^{-1}$)							
	r	0.81^{***}	0.45^{*}	0.00	0.25	0.05	0.47^{*}	-0.47^{*}	0.40^{*}	0.66^{***}
	RMSE	0.476	1.883	0.018	0.016	0.018	0.058	0.032	0.174	0.176
	MAE	0.254	1.419	0.015	0.013	0.016	0.046	0.027	0.139	0.149
	PBIAS%	−3.9	4.3	−27.9	9.8	−11.3	0.5	12.8	9.3	9.1
			Load ($t\ d^{-1}$)	Load ($kg\ d^{-1}$)						
	r		0.52^{**}	0.48^{*}	0.12	0.59^{***}	0.71^{***}	-0.44^{*}	0.52^{**}	0.62^{***}
	RMSE		0.4	2.4	2.2	2.3	9.0	4.2	39.5	42.9
	MAE		0.3	1.9	1.8	2.0	6.4	3.5	29.4	33.1
	PBIAS%		3.9	−30.2	9.4	−10.4	2.5	15.1	9.2	7.6
Validation (July 2009–June 2010)		($m^3\ s^{-1}$)	Concentration ($mg\ L^{-1}$)							
	r	0.88^{***}	−0.23	0.70^{*}	0.68^{*}	0.17	0.75^{**}	−0.31	0.67^{*}	0.78^{**}
	RMSE	0.479	1.656	0.012	0.012	0.008	0.065	0.025	0.159	0.156
	MAE	0.278	1.372	0.011	0.011	0.007	0.060	0.021	0.109	0.097
	PBIAS%	−14.4	−5.3	23.0	−37.2	−0.3	−19.8	15.0	10.8	7.4
			Load ($t\ d^{-1}$)	Load ($kg\ d^{-1}$)						
	r		0.30	0.89^{***}	0.22	0.89^{***}	0.63^{*}	−0.36	0.93^{***}	0.94^{***}
	RMSE		0.3	1.2	2.1	1.9	12.8	3.1	28.5	30.9
	MAE		0.3	1.1	2.0	1.5	9.9	2.7	18.8	20.6
	PBIAS%		−17.2	8.9	−54.9	−14.5	−37.4	10.9	−4.9	−7.6

calibration (9.3% for NO_3–N, 9.1% for TN) and overestimated during validation (4.9% for NO_3–N, 7.6% for TN; Table 2). Higher r values for simulations of NO_3–N and TN loads during calibration ($r \geq 0.52$, $p < 0.01$) and validation ($r \geq 0.93$, $p < 0.001$) were again indicative of the importance of discharge.

3.1.2. DYRESM–CAEDYM model of Lake Rotorua

Most DYRESM–CAEDYM parameter values used in this study were taken from the latest modelling study of Lake Rotorua in Abell et al. (2015) but two were adjusted to better fit observed data. The adjusted parameters included the maximum denitrification rate coefficient, altered from 0.8 to 0.5 d^{-1}, and release rate of NH_4–N from the sediment, altered from 0.2 to 0.3 $g\ m^{-2}\ d^{-1}$. A summary of key parameter values that were optimised by manual calibration in both Abell et al. (2015) and this study is shown in Table 3.

In surface waters of Lake Rotorua (0–6 m deep), variations in nutrient concentrations were generally well reproduced by DYRESM–CAEDYM, including increases in winter and decreases in summer for PO_4–P (identical to the variable DRP simulated by SWAT), NH_4–N and NO_3–N (Fig. 4a, e and g). Simulations of PO_4–P and NH_4–N showed low or negative r values during calibration (January 2008–June 2009) and validation (July 2009–June 2010) and tended to be overestimated (PBIAS ≤ −38.1%) during validation (Table 4). However, the modelled TP concentrations showed reasonable agreement with the observations during calibration ($r = 0.63$; $p < 0.01$) and validation ($r = 0.79$; $p < 0.01$), although concentrations were slightly underestimated, by 12.1% during calibration and 16.5% during validation (Table 4). A highly positive correlation ($r = 0.74$; $p < 0.01$) between simulated and observed concentrations of NO_3–N was found during validation, although values were overestimated (PBIAS = −72.3%; Table 4). Simulated TN concentrations also showed good agreement with observations during both calibration ($r = 0.73$; $p < 0.01$) and validation ($r = 0.81$; $p < 0.01$), with low bias (+6.1% and −2.4%, respectively, Table 4).

Model performance for lake surface Chl a concentrations (Fig. 4k) was poor, showing low r values during calibration ($r = 0.09$, $p > 0.05$) and validation ($r = 0.38$, $p > 0.05$) and Chl a concentrations tended to be underestimated during calibration (PBIAS = 24.1%) and validation (PBIAS = 10.8%; Table 4). The mean TLI3 value was 4.54 for July 2009 to June 2010 based on the measured concentrations of Chl a, TP and TN in surface waters of Lake Rotorua, compared to 4.47 based on the DYRESM–CAEDYM simulation under baseline conditions of both wastewater irrigation and pasture fertilisation (Table 5).

At 19 m depth ("bottom"), simulated nutrient concentrations showed large variations, with peaks corresponding either to periods of hypoxia in the hypolimnion during stratified periods, or intervening isothermal periods, depending on the analyte (Fig. 4). However, the DYRESM–CAEDYM model simulations showed only modest statistical performance with most of the measured nutrient concentrations (range in r values of −0.38 to 0.37 during calibration and validation; Table 4).

Table 3
Sensitive DYRESM–CAEDYM parameter values that were adjusted from Abell et al. (2015).

Parameter	Unit	Calibrated value
Dissolved organic nutrients		
Max. rate of mineralisation of labile dissolved organic phosphorus (DOPL) to phosphate (PO_4–P)	d^{-1}	0.01
Max. rate of mineralisation of labile dissolved organic nitrogen (DONL) to ammonium (NH_4–N)	d^{-1}	0.01
Dissolved inorganic nutrients		
Denitrification rate coefficient	d^{-1}	0.50
Nitrification rate coefficient	d^{-1}	0.10
Nutrient fluxes in sediment		
Release rate of PO_4–P	$g\ m^{-2}\ d^{-1}$	0.02
Release rate of NH_4–N	$g\ m^{-2}\ d^{-1}$	0.30
Release rate of nitrate (NO_3–N)	$g\ m^{-2}\ d^{-1}$	−0.10

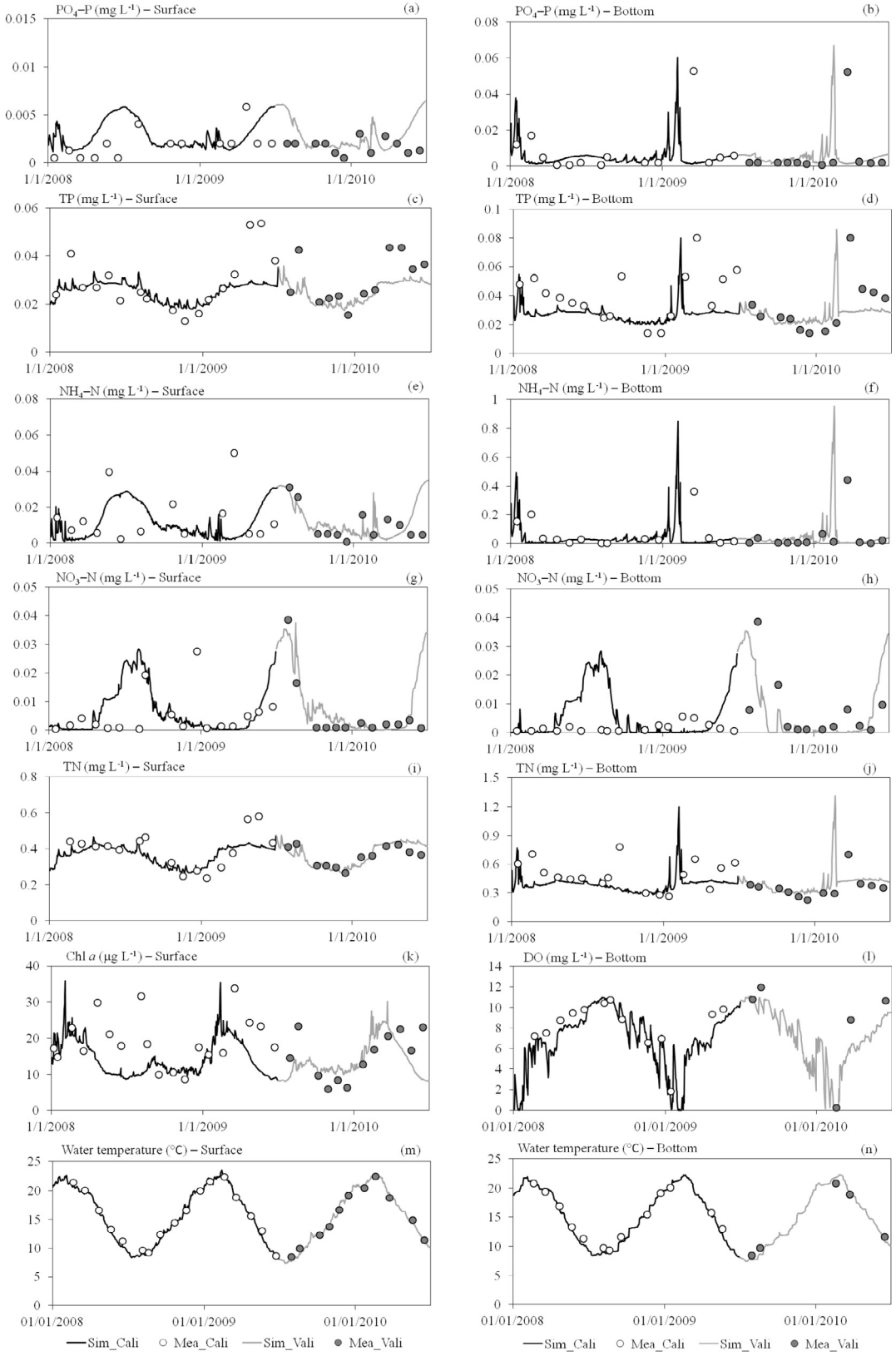

Fig. 4. Comparisons of concentrations simulated with DYRESM–CAEDYM of (a–b) phosphate (PO_4–P), (c–d) total phosphorus (TP), (e–f) ammonium–nitrogen (NH_4–N), (g–h) nitrate–nitrogen (NO_3–N), (i–j) total nitrogen (TN), (k) chlorophyll *a* (Chl *a*), (l) dissolved oxygen (DO), and (m–n) water temperature with the measurements taken at the surface (0–6 m) and the bottom (19 m) water of Lake Rotorua, during calibration (January 2008 to June 2009) and validation (July 2009 to June 2010) period.

Table 4
Model performance of DYRESM–CAEDYM for daily mean water temperature (T), concentrations of phosphate (PO_4–P), total phosphorus (TP), ammonium–nitrogen (NH_4–N), nitrate–nitrogen (NO_3–N) and total nitrogen (TN) for surface (0–6 m) and bottom (19 m) waters of Lake Rotorua, surface water chlorophyll *a* (Chl *a*) and bottom water dissolved oxygen (DO) during calibration (January 2008 to June 2009) and validation (July 2009 to June 2010). Daily mean output from DYRESM–CAEDYM simulations was compared with values measured in the lake at monthly interval on that sampling day. Values of Pearson product moment correlation coefficient (*r*), level of significance (*p*), root mean square error (RMSE), mean absolute error (MAE), and percent bias (PBIAS) were used to indicate model performance. $^{**}p < 0.01$. Units are relevant to RMSE and MAE values only.

Model performance	Statistics	Lake surface waters (0–6 m)							Lake bottom waters (19 m)						
		T	PO_4–P	TP	NH_4–N	NO_3–N	TN	Chl *a*	T	DO	PO_4–P	TP	NH_4–N	NO_3–N	TN
		°C	mg L^{-1}					µg L^{-1}	°C	mg L^{-1}					
Calibration	*r*	0.9986**	0.10	0.63**	−0.15	0.14	0.73**	0.09	0.9987**	0.9374**	0.00	0.19	0.20	−0.38	0.16
(January2008 –June 2009)	RMSE	0.551	0.002	0.010	0.018	0.011	0.074	9.280	0.564	1.327	0.016	0.020	0.138	0.011	0.136
	MAE	0.477	0.002	0.007	0.014	0.006	0.057	7.425	0.492	1.165	0.008	0.015	0.075	0.007	0.136
	PBIAS%	3.0	−63.0	12.1	13.8	−40.1	6.1	24.1	2.6	10.8	25.3	29.0	25.0	−312.7	17.0
Validation	*r*	0.9984**	−0.24	0.79**	0.28	0.74**	0.81**	0.38	0.9995**	0.9694**	−0.16	−0.10	−0.12	0.37	−0.07
(July2009 –June 2010)	RMSE	0.620	0.002	0.008	0.012	0.009	0.035	6.338	0.832	1.517	0.023	0.024	0.273	0.012	0.281
	MAE	0.571	0.002	0.006	0.009	0.006	0.029	5.054	0.811	1.214	0.012	0.017	0.132	0.008	0.150
	PBIAS%	2.3	−76.1	16.5	−38.1	−72.3	−2.4	10.8	1.2	13.0	−60.2	0.9	−109.6	3.4	−26.5

Simulated concentrations of PO_4–P and NH_4–N in bottom waters were highest during summer thermal stratification (Fig. 4b, f), which coincided with the period of occasional hypolimnetic anoxia. A positive correlation ($r = 0.37$; $p > 0.05$) between simulated and observed concentrations of NO_3–N (PBIAS = 3.4%) was found during validation (Table 4). The highest simulated concentrations of NO_3–N occurred in winter when the water column was continuously well mixed (Fig. 4h). When the water column was stratified for periods of up to several days, both modelled and observed TP at 19 m depth predominantly comprised PO_4–P (Fig. 4b, d) and TN predominantly comprised NH_4–N (Fig. 4f, j). Modelled TP concentrations showed poor agreement with the observations ($r = 0.19$; $p > 0.05$) during calibration and were underestimated by 29.0% (Table 4).

Model performance for lake bottom DO concentrations (Fig. 4l), and lake surface and bottom water temperatures (Fig. 4m and n) was very good, showing high *r* values during calibration and validation ($r > 0.99, p < 0.01$; Table 4). Concentrations of DO in bottom waters of Lake Rotorua were slightly underestimated, by 10.8% during calibration and 13.0% during validation (see PBIAS in Table 4). Simulated surface and bottom water temperatures showed low bias (≤3%) during both calibration and validation (Table 4).

Measurements at monthly intervals and simulated concentrations on corresponding days in the surface and bottom waters of Lake Rotorua under the current climate (CC0) during calibration (January 2008–June 2009) and validation (July 2009–June 2010) are also compared in Fig. 5, showing larger variances in the measured data than the simulated results.

3.2. Catchment and lake scenarios: current climate

Under the reference scenario (S1–Irr1Pas1) corresponding to current climate, 65 t yr^{-1} of P was applied to the Puarenga catchment from July 2006 to June 2010; 61.5% (40 t yr^{-1}) as pastoral fertiliser and 38.5% (25 t yr^{-1}) as irrigated wastewater (Table 6). As part of these applications, 180 t yr^{-1} of N was also applied; 70.6% (127 t yr^{-1}) as pastoral fertiliser and 29.4% (53 t yr^{-1}) as irrigated wastewater (Table 6).

Mean TP and TN loads at the FRI stream–gauge for the four years of the SWAT simulation (July 2006–June 2010; baseline period) varied among the four nutrient application scenarios relative to the current climate condition (CC0). For S1–Irr1Pas1, the TP load at the FRI stream–gauge was 4.3 t yr^{-1} (Table 6), indicating that 93.4% of the 65 t yr^{-1} applied to land from wastewater irrigation and pasture fertilisation was attenuated and therefore not exported downstream during

Table 5
Measured sampling days and corresponding simulation days with changes in surface and bottom water temperature (ΔT) > 0.5 °C, with bottom water dissolved oxygen (DO) concentrations < 2 mg L^{-1}, and with surface water chlorophyll *a* (Chl *a*) concentrations > 15 µg L^{-1}, and TLI3 values under the current climate during calibration (2008–2009) and validation (2009–2010), daily simulated number of days with ΔT > 0.5 °C, DO < 2 mg L^{-1}, Chl *a* > 15 µg L^{-1}, and mean TLI3 values under current climate (CC0) relative to four nutrient load scenarios (S1–S4) during baseline period (2008–2010), and under 2090 climate changes to catchment only (CC1) and changes to both catchment and lake (CC2). Nutrient load scenarios are described in the Methods. The TLI3 is a three–variable Trophic Level Index function derived from concentrations of total nitrogen, total phosphorus and Chl *a*, which is used to indicate the lake trophic state (Burns et al., 1999).

	CC0: S1–Irr1Pas1 (monthly values)				CC0: S1–S4 (daily values)				CC1: catchment only (daily values)	CC2: catchment & lake (daily values)
	Calibration: 2008–2009		Validation: 2009–2010		Baseline: 2008–2010				Future: 2090	Future: 2090
	Measured	Simulated	Measured	Simulated	S1–Irr1Pas1	S2–Irr0Pas1	S3–Irr1Pas0	S4–Irr0Pas0	S2–Irr0Pas1	S2–Irr0Pas1
	Number of days (d)		Number of days (d)		Number of days (d)				Number of days (d)	Number of days (d)
ΔT > 0.5 °C	5	3	1	2	316	294	308	291	303	345
Bottom DO < 2 mg L^{-1}	1	1	1	1	75	58	62	53	70	141
Surface Chl *a* > 15 µg L^{-1}	10	4	4	1	306	291	296	291	301	446
mean TLI3	4.68	4.5	4.54	4.47	4.49	4.46	4.46	4.44	4.46	4.88

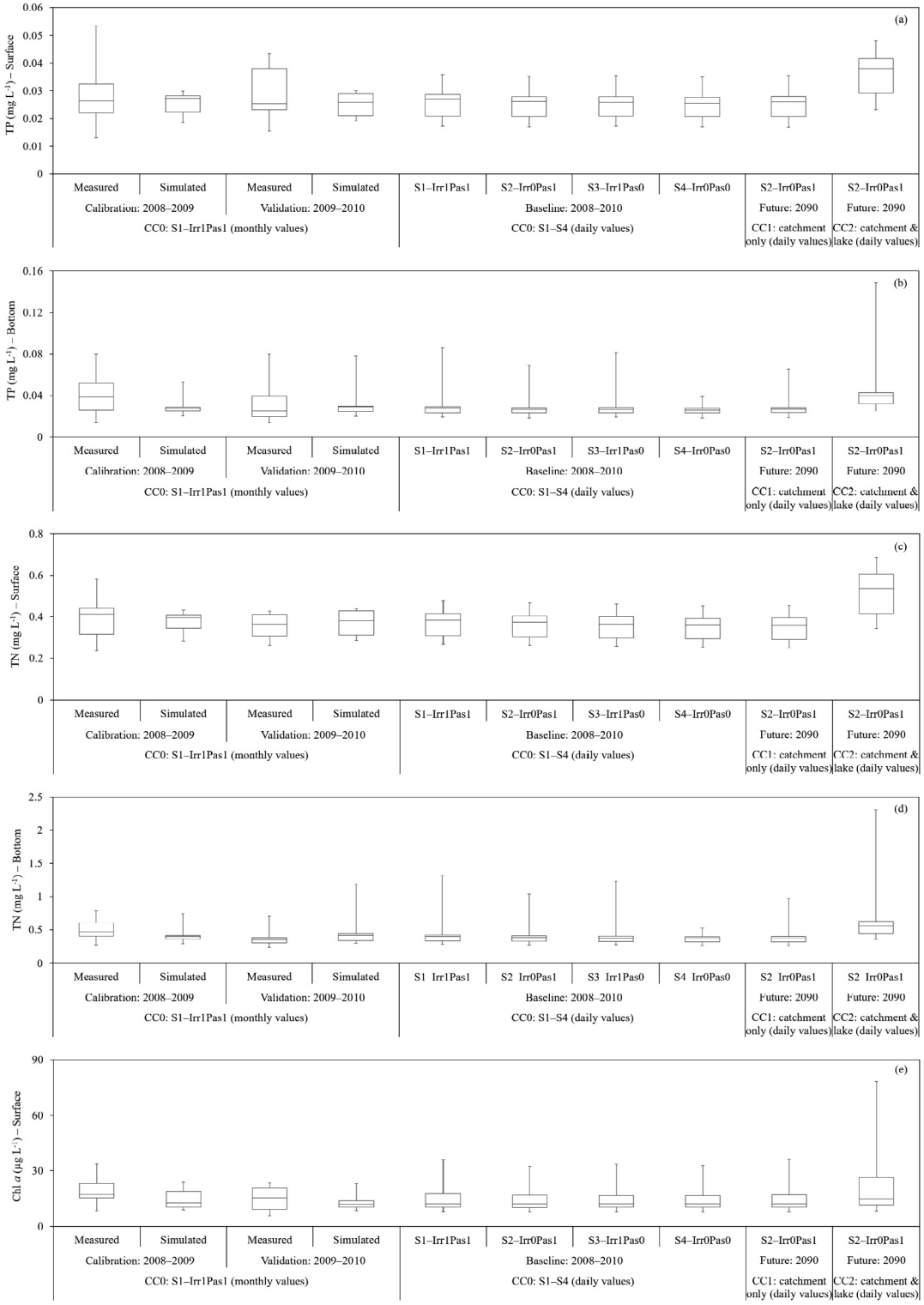

Fig. 5. Measurements at monthly intervals and simulated concentrations on corresponding days in the surface and bottom waters of Lake Rotorua under the current climate (CC0) during calibration (2008–2009) and validation (2009–2010); daily simulated concentrations in the surface and bottom waters of Lake Rotorua under current climate (CC0) relative to four nutrient load scenarios (S1–S4) during a baseline period (2008–2010), and under 2090 climate changes to catchment only (CC1) and changes to both catchment and lake (CC2). (a)–(b) TP: total phosphorus, (c)–(d) TN: total nitrogen, and (e) Chl *a*: chlorophyll *a*. Nutrient load scenarios are described in the Methods. Boxes denote interquartile ranges (i.e., 25% and 75%); whiskers denote minimum and maximum values; horizontal lines denote median values.

that period. The application of pastoral fertiliser alone (S2–Irr0Pas1) resulted in an in–stream TP load of 3.7 t yr^{-1} (Table 6), a reduction of 14.0% from the simulations under S1–Irr1Pas1. The scenario comprising only wastewater irrigation (S3–Irr1Pas0) resulted in an annual TP load of 2.9 t yr^{-1} (Table 6), a 32.6% reduction from simulations of TP under S1–Irr1Pas1. Simulations with no nutrient application (S4–Irr0Pas0) reduced the in–stream annual TP load by 39.5% (2.6 t yr^{-1}; Table 6) from the load under S1–Irr1Pas1.

Table 6
Model results under current climate (CC0) for four nutrient load scenarios comprising changes to total phosphorus (TP) and total nitrogen (TN) loads from the Puarenga Stream catchment and in–stream TP and TN loads during baseline period (July 2006 to June 2010); changes to TP and TN concentrations in surface and bottom waters, and surface water chlorophyll *a* (Chl *a*) concentrations of Lake Rotorua during the baseline period (January 2008 to June 2010). Percentage change denotes changes to the simulations under scenarios S2–S4 relative to the simulations under the "reference" scenario S1. Nutrient load scenarios (S1–S4) are described in the Methods. S1–Irr1Pas1: both nutrient applications, S2–Irr0Pas1: pasture fertilisation only, S3–Irr1Pas0: wastewater irrigation only, S4–Irr0Pas0: no nutrient applications.

Scenarios	TP				TN				Chl *a*
	Applied to catchment ($t\ yr^{-1}$)	In–stream load to lake ($t\ yr^{-1}$)	Surface of lake ($mg\ L^{-1}$)	Bottom of lake ($mg\ L^{-1}$)	Applied to catchment ($t\ yr^{-1}$)	In–stream load to lake ($t\ yr^{-1}$)	Surface of lake ($mg\ L^{-1}$)	Bottomof lake ($mg\ L^{-1}$)	Surface of lake ($\mu g\ L^{-1}$)
S1–Irr1Pas1	65	4.3	0.0254	0.0275	180	62.9	0.368	0.394	14.178
S2–Irr0Pas1	40	3.7	0.0248	0.0262	127	46.7	0.358	0.373	13.731
S3–Irr1Pas0	25	2.9	0.0248	0.0263	53	31.8	0.353	0.369	13.775
S4–Irr0Pas0	0	2.6	0.0245	0.0256	0	15.6	0.347	0.357	13.597
	% change				% change				% change
S1–Irr1Pas1 vs. S2–Irr0Pas1	−38.5	−14.0	−2.4	−4.7	−29.4	−25.8	−2.7	−5.3	−3.2
S1–Irr1Pas1 vs. S3–Irr1Pas0	−61.5	−32.6	−2.4	−4.4	−70.6	−49.4	−4.1	−6.3	−2.8
S1–Irr1Pas1 vs. S4–Irr0Pas0	−100.0	−39.5	−3.5	−6.9	−100.0	−75.2	−5.7	−9.4	−4.1

The mean simulated in–stream TN load at the FRI stream–gauge over the four–year simulation for S1–Irr1Pas1 was 62.9 $t\ yr^{-1}$ (Table 6), representing an attenuation of 65.1% of the TN load applied from wastewater irrigation and pasture fertilisation (S1–Irr1Pas1; 53 and 127 $t\ yr^{-1}$, respectively). The applications of S2–Irr0Pas1, S3–Irr1Pas0, S4–Irr0Pas0 resulted in a four–year annual mean in–stream TN load of 46.7, 31.8 and 15.6 $t\ yr^{-1}$, respectively (Table 6). These three scenarios represent respective reductions of 25.8%, 49.4%, and 75.2% (Table 6) relative to simulations under the reference scenario S1–Irr1Pas1.

For the DYRESM–CAEDYM simulations of 2.5 years (January 2008–June 2010; baseline period), annual mean concentrations of TP and TN in the surface and bottom waters and Chl *a* in surface waters are similar for the different nutrient application scenarios (S1–S4) under current climate (CC0) (see Fig. 5), as well as the mean TLI3 value (see Table 5). Annual mean TP concentrations at the lake surface under the catchment scenarios of S2–Irr0Pas1, S3–Irr1Pas0, and S4–Irr0Pas0 were slightly reduced, by 2.4%, 2.4%, and 3.5% (Table 6), respectively, compared with the annual mean (0.0254 $mg\ L^{-1}$) under S1–Irr1Pas1 (Table 6). Annual mean TP concentration at the lake bottom under the catchment scenarios of S2–Irr0Pas1, S3–Irr1Pas0, and S4–Irr0Pas0 declined slightly, by 4.7%, 4.4%, and 6.9% (Table 6), respectively, compared with the value of 0.0275 $mg\ L^{-1}$ at the lake bottom under S1–Irr1Pas1 (Table 6). Annual mean TN concentrations at the lake surface under the catchment scenarios of S2–Irr0Pas1, S3–Irr1Pas0, and S4–Irr0Pas0 declined slightly, by 2.7%, 4.1%, and 5.7% (Table 6), respectively, compared with 0.0368 $mg\ L^{-1}$ at the lake surface under S1–Irr1Pas1 (Table 6). Annual mean TN concentrations at the lake bottom under the catchment scenarios of S2–Irr0Pas1, S3–Irr1Pas0, and S4–Irr0Pas0 also declined slightly, by 5.3%, 6.3%, and 9.4% (Table 6), respectively, compared with 0.0394 $mg\ L^{-1}$ at the lake bottom under S1–Irr1Pas1 (Table 6). Annual mean Chl *a* concentration at the lake surface under the catchment scenarios of S2–Irr0Pas1, S3–Irr1Pas0, and S4–Irr0Pas0 declined slightly, by 3.2%, 2.8%, and 4.1% (Table 6), respectively, compared with 14.178 $\mu g\ L^{-1}$ at the lake surface under S1–Irr1Pas1 (Table 6).

Decreases in nutrient loads in the Puarenga Stream under scenario S4–Irr0Pas0 gave reductions in total external loads from the whole Rotorua catchment of only 6.2% for TP and 11.3% for TN. Given that the changes were only made to 15.6% of TP load and 16.2% of TN load contributing to Lake Rotorua, large changes in water quality of the whole lake would not be expected, i.e., ~84% of the TP and TN input remained unchanged.

3.3. Catchment and lake scenarios: 2090 climate

Two climate change scenarios were simulated to predict changes to lake trophic state in response to a projected future climate of 2090. The first considered the effects of 2090 climate forcing on discharge and nutrient loadings from the catchment but simulated the lake with meteorological input data from a current (2006–10) climate. The second used 2090 climate data as input to both the catchment and the lake models. This study design was intended to isolate the impact on lake water quality of projected future climate effects on catchment processes (e.g., altered discharge and nutrient fluxes) from projected future climate effects directly on the lake (e.g., increased phytoplankton growth rates due to elevated temperature). For the 2090 climate impact on the catchment only (CC1) and on both catchment and lake (CC2), scenario S2–Irr0Pas1 was applied for other streams and on the lake (see details in Subsection 2.4.2).

3.3.1. Effects of climate change on catchment discharge, suspended solids and nutrient loads

For the projected future climate of 2090 (IPCC, 2013), annual mean precipitation and solar radiation are projected to increase by 2.8% and 1.4%, respectively, humidity to decrease by 0.6%, and air temperature to increase by 2.7 °C. For precipitation, the largest increase will be in the month of March and the largest decrease will be in October.

Relative to the scenario S2–Irr0Pas1, for each sub–catchment discharge and SS loads increased by 4.6% and 3.8%, respectively, under the 2090 climate scenario (Table 7). Nutrient loads increased with the exception of NO_3–N and TN. The largest load increases were 14.4% for NH_4–N load, followed by 6% for DRP, ORGP, TP and 5.8% for ORGN. The largest load decrease was 13.4% for NO_3–N, which was mostly responsible for a decrease in TN load by 7.6%. A 2090 climate generally resulted in large increases in discharge, suspended solids and nutrients from January to April, and small increases from May to September (Table 7). Increases were greatest in March; 11.1% for discharge, 11.5% for SS load, 15.3% for ORGP, 10.4% for TP, and 14.3% for ORGN. For dissolved nutrient species loads, decreases of NO_3–N were greatest in September (28%), and increases of DRP (7.5%) and NH_4–N (15.7%) were greatest in July.

Relative to the scenario S2–Irr0Pas1, the 2090 climate scenario (i.e.,

Table 7
Changes in inflow (Q) and nutrient loadings of suspended sediment (SS), mineral phosphorus (MINP), organic P (ORGP), ammonium–N (NH_4–N), nitrate–N (NO_3–N), organic N (ORGN), total P (TP), and total N (TN) in response to the 2090 climate impacts on catchment only, and changes of nutrient concentrations in Lake Rotorua. The value of TLI3, the three–variable Trophic Level Index calculated by concentrations of TN, TP and chlorophyll *a* (Chl *a*), is used to indicate the lake trophic state (Burns et al., 1999). The colour scale was specified for each variable in each column and indicates the range of % changes.

Month	Changes in inflow discharge and loadings (%)									Changes in lake concentration (%)					TLI3
										Surface (0–6 m)			Bottom (19 m)		
	Q	SS	DRP	ORGP	NH_4–N	NO_3–N	ORGN	TP	TN	TP	TN	Chl *a*	TP	TN	
Jan	9.5	9.7	5.8	10.2	14.6	-1.3	9.8	7.9	3.5	0.4	-2.5	4.5	-3.6	-6.3	
Feb	9.1	9.4	6.7	13.9	13.6	-6.7	12.8	10.0	0.9	1.1	-1.4	5.2	6.8	4.3	
Mar	11.1	11.5	6.5	15.3	15.7	-10.5	14.3	10.4	-1.7	1.4	-1.3	3.5	1.6	-1.1	
Apr	8.8	10.0	5.8	13.0	15.2	-11.5	12.3	9.3	-4.2	0.3	-2.1	0.1	0.4	-2.1	
May	2.9	2.0	5.9	5.0	15.0	-10.7	4.9	5.4	-6.3	0.1	-2.6	-1.3	0.2	-2.6	
Jun	2.0	1.2	5.6	2.5	14.7	-11.5	2.6	3.8	-7.8	0.2	-3.0	-1.0	0.2	-3.0	
Jul	3.1	2.0	7.5	4.2	15.7	-12.7	4.2	5.5	-8.4	-0.4	-4.1	0.1	-0.4	-4.0	
Aug	4.2	3.3	7.0	4.7	15.1	-14.1	4.7	5.6	-9.6	-0.4	-4.8	-0.6	-0.9	-4.8	
Sep	2.0	0.2	6.3	3.7	13.1	-28.0	3.6	4.9	-19.5	-0.5	-5.6	-0.6	-0.8	-5.1	
Oct	-1.3	-3.5	5.1	-1.4	14.0	-22.6	-1.1	1.6	-17.2	-0.3	-5.5	1.0	1.2	-3.6	
Nov	5.1	3.8	4.4	4.7	13.2	-3.2	4.5	4.6	0.6	0.0	-4.1	0.6	1.2	-3.1	
Dec	4.8	3.5	5.0	6.3	13.2	-5.1	6.0	5.6	-0.4	-0.1	-3.4	4.1	5.8	1.5	
Annual	**4.6**	**3.8**	**6.0**	**6.0**	**14.4**	**-13.4**	**5.8**	**6.0**	**-7.6**	**0.2**	**-3.0**	**1.9**	**0.9**	**-2.3**	**4.46**
%	**-30**													**30**	

2090 climate applied to the catchment model but current climate applied to the lake model; CC1) was predicted with DYRESM–CAEDYM to cause relatively minor changes in Lake Rotorua water quality (see Tables 5 and 7). Periods of lake thermal stratification indicated by the number of days with changes in surface and bottom water temperatures (ΔT) greater than 0.5 °C (Losordo and Piedrahita, 1991) under current climate (CC0) were similar to the periods of thermal stratification under 2090 climate applied only to the catchment (CC1) (see Table 5). Minimal changes were also found to the number of days with DO concentrations in bottom waters $< 2\ mg\ L^{-1}$ (i.e., a threshold for depletion of DO; Stuber et al., 1982) and the number of days with Chl *a* concentrations in surface waters $> 15\ \mu g\ L^{-1}$ (i.e., a threshold for cold water fisheries; McGhee, 1983) under CC0 and CC1 for the catchment (Table 5).

Under the 2090 climate scenario (CC1), annual mean TN concentration decreased by 3.0% in lake surface waters and 2.3% in bottom waters (Table 7), with the largest monthly decrease in surface waters in September (5.6%) and in bottom waters in January (6.3%). Small increases were predicted in annual mean TP concentrations in the lake surface (0.2%) and bottom (0.9%) waters. Small increases (1.9%) were predicted in annual mean Chl *a* concentrations in the lake surface by 2090 (Table 7). Relative to the scenario S2–Irr0Pas1, applying the climate change scenario (CC1) to the catchment model (but not the lake model) yielded a negligible change in the mean TLI3 value (Table 5).

3.3.2. *Effects of climate change on catchment and lake water quality*

Under the projected future climate of 2090, annual mean evaporation is predicted by the lake model to increase by 10.6% (Table 8). For the surface water catchment, annual mean inflow water temperature simulated by the SWAT2012 model increases by 2 °C. For the groundwater recharge catchment, inflow water temperature increases by 2.4 °C (quantified by 88% of the projected increase in air temperature; Kurylyk et al., 2013). Generally, the largest increases in water temperatures for surface water and groundwater were from January to April (Table 8).

Relative to the scenario S2–Irr0Pas1, more frequent and longer periods of thermal stratification were simulated by DYRESM–CAEDYM for Lake Rotorua in 2090 (see Table 5), indicated by the number of days with $\Delta T > 0.5$ °C increasing from 294 (under CC0) to 345 (under CC2). The number of days with DO concentrations in bottom waters $< 2\ mg\ L^{-1}$ was predicted to increase 2.4–fold from 58 (under CC0) to 141 (under CC2), while the number of days with Chl *a* concentrations in surface waters $> 15\ \mu g\ L^{-1}$ was predicted to increase 1.5–fold from 291 (under CC0) to 446 (under CC2).

Applying the combined catchment–lake model simulations using forcing data for a projected 2090 climate gave an increase in annual mean TP, TN and Chl *a* concentrations in lake surface waters of 45.9%, 44.5% and 44.9%, respectively (Table 8), compared with concentrations under the current climate (CC0). The largest increase was in March for TP (57.5%) and February for TN (56.9%) in lake surface waters. For Chl *a* in surface waters, the largest increase was in January (109%) and the smallest increase was in July (4.2%). For bottom waters TP and TN concentrations increased by 56.4% and 56.8%, respectively (Table 8). The largest increase occurred in February for TP (141.1%) and TN (152.0%) in bottom waters.

The 2090 climate scenario applied to the catchment and the lake model gave a substantial increase in the mean TLI3 value from 4.46 (current climate) to 4.88 (Table 5). Fig. 5 shows the major changes in annual mean concentrations of TP and TN in the surface and bottom waters and Chl *a* in surface waters of Lake Rotorua between the 2090 climate on the catchment only (CC1) and on both the catchment and lake (CC2).

4. Discussion

This study integrated catchment discharge and nutrient concentrations from the SWAT2012 model with the lake water quality model DYRESM–CAEDYM, yielding a quantitative assessment of the effects of land management practices and future climate change on trophic state of a nationally iconic lake in New Zealand. Simulation of a range of nutrient load and climate scenarios using a factorial study design allowed the relative effects of land management and projected climate change to be examined. Further, the effects of projected climate change on lake water quality were then examined to isolate the effects due to

Table 8
Precipitation (PCP), solar radiation (SLR), air temperature (T_a), humidity (HMD), evaporation (E_a), water temperatures of inflows from groundwater discharge sub–catchments (T_{gw}) and from surface water sub–catchments (T_{sw}), and changes in nutrient concentrations in Lake Rotorua in response to a projected 2090 climate, for both Lake Rotorua catchment and lake. The increase in T_{gw} was 88% of the increase in T_a while the increase in T_{sw} was from the SWAT output. The TLI3 is a three–variable Trophic Level Index function derived from concentrations of total nitrogen (TN), total phosphorus (TP) and chlorophyll *a* (Chl *a*), which used to indicate the lake trophic state (Burns et al., 1999). The colour scale was specified for each variable in each column and indicates the range of % change.

Month	Absolute changes in inflow water temperature (°C)		Changes for water balance calculations (%)					Changes in concentration (%)					
								Lake surface			Lake bottom		TLI3
	$^*T_{gw}$	$^*T_{sw}$	$^*T_a$	SLR	HMD	E_a	PCP	TP	TN	Chl *a*	TP	TN	
Jan	2.8	2.4	3.2	1.1	-0.7	8.6	5.0	48.0	46.3	109.9	56.0	58.7	
Feb	2.6	2.3	3.0	0.7	-1.4	7.7	6.0	56.9	56.9	98.7	141.1	152.0	
Mar	2.7	2.3	3.1	0.7	0.0	10.0	12.7	57.5	56.3	52.2	61.1	60.1	
Apr	2.5	2.1	2.8	1.2	-0.7	20.4	6.9	51.7	52.8	28.1	52.6	53.7	
May	2.4	2.0	2.7	1.8	-0.4	21.5	3.4	48.4	49.8	17.5	48.4	49.9	
Jun	2.3	1.9	2.6	2.2	-0.3	20.9	3.6	45.6	46.3	9.0	45.6	46.3	
Jul	2.4	2.0	2.7	0.9	-0.3	12.2	2.2	39.7	38.5	4.2	39.7	38.5	
Aug	2.4	2.0	2.7	1.0	0.0	12.8	4.9	36.9	32.2	16.6	36.8	32.8	
Sep	2.1	1.8	2.4	2.4	-0.1	9.6	-4.1	34.5	28.7	9.4	32.9	28.8	
Oct	2.2	1.9	2.5	2.8	-0.6	5.9	-7.8	34.2	28.1	6.2	35.5	30.4	
Nov	2.1	1.8	2.4	1.4	-1.1	8.1	-0.5	33.2	29.0	15.8	37.7	32.3	
Dec	2.3	1.9	2.6	1.0	-1.2	7.1	-1.7	38.2	35.1	42.6	45.1	42.0	
Annual	**2.4**	**2.0**	**2.7**	**1.4**	**-0.6**	**10.6**	**2.8**	**45.9**	**44.5**	**44.9**	**56.4**	**56.8**	**4.88**
	-3	**3**	**-25**				**25**	**-150**				**150**	

catchment processes, from those due to in–lake processes. The results show that the effects on lake water quality due to major changes to nutrient loading in one sub–catchment are minor relative to the effects due to changes to in–lake processes associated with projected climate change.

4.1. Model performance and sensitivity

The improved SWAT2012 model performed better than SWAT2009 (see Me et al., 2015) for simulating concentrations of TN and TP in the Puarenga Stream. For the validation period, discharge and loads of TP and TN from the Puarenga Stream catchment simulated using the SWAT2012 model generally showed positive correlations ($r \geq 0.88$, $p < 0.001$) with the measured data, but less so for in–stream concentrations of TN ($r = 0.78$, $p < 0.01$) and TP ($r = 0.17$, $p > 0.05$). Overestimates of discharge in Puarenga Stream during high rainfall in winter could be due to overestimates of lateral flow contributions (Cartwright et al., 2014). The relatively high value of parameter slope steepness (HRU_SLP), assigned as 0.1 (equal to 5.7° slope based on the average DEM slope) and applied over the entire catchment in this study, may have resulted in overestimates of lateral flow contributions from shallow aquifers to stream channels (Ward et al., 2012).

Periods of elevated discharge are also important because they correspond to increased nutrient mobilisation and erosive processes operating at the landscape scale (Abell et al., 2013). Poor model performance for simulations of DRP and TP concentrations could be partly related to the SWAT2012 soil P parameters, which are lumped for the catchment, such as PSP (P availability index), PHOSKD (soil P partitioning coefficient) and PPERCO (soil P percolation coefficient) (Arnold et al., 2013). Ideally, parameter values should also be optimised to reflect episodic events (Zhang et al., 2015), dry and wet periods, and relevant irrigation regimes such as in the forestry–harvested area in this study. It is possible, therefore, that the values of these parameters do not accurately represent P transport on the landscape following rainfall.

Seasonal variations in concentrations of N species from the Puarenga Stream catchment were well simulated by SWAT2012. Higher simulated concentrations of NH_4–N occurred in summer, likely due to the increased temperature in this season, which enhances rates of organic mineralisation processes (Hien et al., 2016). The underestimation of NH_4–N concentrations in winter could have also resulted from overestimates of discharge in Puarenga Stream during high rainfall in winter (i.e., dilution). Higher concentrations of NO_3–N simulated in winter reflect the higher leaching rates of NO_3–N when the soils become saturated following high rainfall, resulting in high rates of leaching to the stream. Simulated NO_3–N concentrations were lower than observed values in summer, probably because of the inability of SWAT to adequately replicate the relative increase in NO_3–enriched groundwater flow to the channel (Bain et al., 2012). This highlights the importance of enhancing SWAT performance by improving the representation of interactions between the groundwater aquifer and river channel, which represents a critical area for nutrient dynamics (Guzman et al., 2015).

The lake model (DYRESM–CAEDYM) predictions for surface waters showed strong seasonality that was similar to the measured data, with high positive correlations between measured and simulated TP and TN concentrations. Polymictic, temperate lakes mix intermittently during the summer stratified period in response to wind (Kourzeneva et al., 2012) and this was both observed and simulated in this study. Brief spikes of PO_4–P and NH_4–N concentrations observed in lake surface waters in summer were well simulated due to the ability of the model to capture wind–driven lake–turnover events. The accumulated nutrients and increased temperature during this period concurrently accelerated phytoplankton growth, with simulated surface concentrations of Chl *a* (a proxy for phytoplankton biomass) generally highest in summer. However, poor model performance for simulating Chl *a* concentrations may be due to inadequate representation of the ecology of key phytoplankton guilds. Also, spatial variations in surface chlorophyll *a* concentrations can be particularly large in Lake Rotorua (Allan et al., 2011) and therefore there is large sampling error when comparing spot measurements from central lake sites with horizontally–averaged predictions from a 1–D model. In general, DYRESM–CAEDYM reproduced

the temporary stratification and deoxygenation events that lead to release of PO_4–P and NH_4–N from the bottom sediments (Hamilton et al., 2004; Burger et al., 2007a). The annual maximum of PO_4–P, NO_3–N and NH_4–N concentrations in surface waters was both observed and simulated during winter, which could be attributed to higher rainfall during this season, transporting more nutrients into the lake (Abell et al., 2013), as well as lower nutrient uptake rates associated with lower temperature and reduced light availability.

4.2. Reducing nutrient loads to the Puarenga Stream catchment

Nutrient loads to the Puarenga Stream decreased under the different nutrient load reduction scenarios. Under the scenario of wastewater removal (S2–Irr0Pas1), the reduction (38.5%) in the applied TP load was larger than the reduction (14.0%) in in–stream TP load. This finding could be explained by the high soil P adsorption rate (PSP was set to 0.6; mean value derived from Beets et al., 2013). Loads of TN in the farmland–applied fertiliser were 2.4 times higher than those associated with the applied wastewater, and consequently simulations of in–stream annual TN loads under the scenario S2–Irr0Pas1 were 1.5 times higher than those under the scenario of farmland–applied fertiliser removal (S3–Irr1Pas0). The difference indicates there is also some loss of N between where it is applied and the stream, which may be attributed to processes such as plant uptake and export of N in production, as well as denitrification. This is supported by the modelled outputs showing 1) the reduction (82.3%) of plant uptake of N in the Puarenga Stream catchment under the scenario of farmland–applied fertiliser removal (S3–Irr1Pas0) was larger than the reduction (5.1%) under the scenario of wastewater removal (S2–Irr0Pas1); 2) the reduction (80.1%) of nitrate–nitrogen yield in lateral flow under the scenario of farmland–applied fertiliser removal (S3–Irr1Pas0) was larger than the reduction (14.8%) under the scenario of wastewater removal (S2–Irr0Pas1); and 3) the reduction (80.5%) of N from denitrification under the scenario of farmland–applied fertiliser removal (S3–Irr1Pas0) was larger than the reduction (14.3%) under the scenario of wastewater removal (S2–Irr0Pas1). Without any anthropogenic nutrient loadings (S4–Irr0Pas0), there was a moderate reduction of in–-stream annual TP load (39.5%) and a large reduction of in–stream annual TN load (75.2%). The difference between N and P may be attributed to the high soil P adsorption rate (PSP; 0.6), resulting in a legacy of P (see Sharpley et al., 2014) being retained in the catchment soils. By contrast, the relatively rapid leaching of N reflects the mobile nature of this nutrient (Zogg et al., 2000) with high N percolation rate assigned in the SWAT model (NPERCO; 0.05).

The scenario without any anthropogenic nutrient loadings from the Puarenga Stream catchment (i.e., S4–Irr0Pas0) was predicted to cause minimal improvement to lake water quality. Simulated nutrient reductions in the Puarenga Stream catchment are a minor fraction of total catchment nutrient load to Lake Rotorua and TP and TN loads remain largely unchanged. In the short term, the benefits from external nutrient load reductions may be difficult to decipher unless they are large in magnitude relative to internal loading. For shallow, polymictic Lake Rotorua, periods of thermal stratification, of sufficient duration to generate hypoxia, lead to large nutrient releases to bottom waters (Burger et al., 2007a) and are interspersed with mixing events that make these nutrients available to support phytoplankton production in euphotic waters.

4.3. Climate change impacts on catchment and lake

Predictions from the combined climate–catchment model indicate that there would be increases in discharge, and loads of SS, and especially particulate N and P, mostly from January to April for a 2090 climate. This could be explained by the elevated rates of soil erosion and mobilisation of particulate P and N associated with increased frequency of intense rainfall events which generate quick flow. Decreases in simulated discharge during October reflect small projected declines in precipitation during the Austral spring. Overall, the modelled increase in mean stream discharge (4.6%) in response to the projected increase in precipitation (2.8%) for a 2090 climate will reflect the soil, topography and land cover in the Puarenga Stream catchment, which has mostly pumice soils, moderate slope (5.7°), and extensive areas of forest (47%). Our approach of applying modelled changes for the Puarenga Stream catchment to other sub–catchments was appropriate to provide a synoptic assessment, although the precise response of stream discharge to changes in precipitation will vary somewhat in other sub–catchments. In general, discharge may increase to a greater extent in sub–catchments with higher proportions of pasture; however, this will depend on other factors such as the dominance of groundwater contributions and catchment slope.

Elevated soil temperature and in–stream water temperature in 2090 would increase decomposition and mineralisation of organic matter, which could then increase DRP and NH_4–N loads. Hien et al. (2016) predicted that NH_4–N loads would increase in almost all months of the year in response to projected future climate warming, an effect that they attributed to organic mineralisation processes. Large decreases in NO_3–N load occurred in September and October under projected climate change, which corresponded to a period of decreased precipitation in these months. Loads of NO_3–N also decreased from January to August 2090 during a period of increased precipitation, indicating that elevated soil temperature due to warming would increase plant uptake and denitrification processes, causing a decrease in NO_3–N loads and leaching from the catchment. This is consistent with N simulation results in Arheimer et al. (2012), who modeled climate change impacts on riverine nutrient loads to the Baltic Sea. They similarly predicted decreased NO_3–N losses associated with climate change, which they attributed to plant uptake and denitrification processes.

Donnelly et al. (2011) predicted that TN load from the Vistula River catchment (Poland; 325 km^2; 63% agricultural land use) would decrease by 4% under increased temperature due to global warming. In the Puarenga Stream catchment, 47% of the land use is exotic *Pinus radiata* forest, and therefore plant uptake could play the primary role in reducing TN loads from the catchment; TN loads decreased 7.6% under the 2090 climate in our study. For 10 catchments (areas 4.36–41.91 km^2) in the north of Denmark with similar rainfall to our study area, predicted increases in TP loads ranged from 3.3% to 16.5% by 2100 (Jeppesen et al., 2009). Increases in TP load (6%) predicted for the Puarenga Stream catchment in 2090 were small compared to values given by Jeppesen et al. (2009), and may reflect high soil P adsorption in soils of this catchment (Beets et al., 2013) and correspondingly high P adsorption rate (0.6) in the model. The contrasting response of catchment TN and TP loads to projected climate change likely reflects the relatively rapid mobilisation of N through leaching, while P is mostly retained in the soils. Under the 2090 climate applied to the catchment only, there was a decrease (3.0%) in annual mean TN concentration in lake surface waters but an increase (1.9%) in annual mean Chl *a* concentrations, highlighting the potential that redox dynamics of N in the bottom waters could be changed by the decreased external NO_3–N load (Burger et al., 2008).

For shallow, polymictic Lake Rotorua, increased water temperatures in 2090, with frequent and longer periods of summer thermal stratification and bottom water deoxygenation, are consistent with previous models of this lake (Özkundakci et al., 2012) and lakes elsewhere (e.g., Wilhelm and Adrian, 2008). The stratification–deoxygenation effect was well–predicted by DYRESM–CAEDYM under baseline conditions. An increase in temperature will also enhance the mineralisation of organic matter as well as causing higher rates of sediment nutrient release (e.g., NH_4–N and PO_4–P) from bottom sediments (Adrian et al., 2009). These two inorganic nutrient species (NH_4–N and PO_4–P) have been found by Burger et al. (2008) to be the dominant source of increases in N and P concentrations in surface waters of Lake Rotorua when there are mixing events following extended stratification periods during

summer. Burger et al. (2008) also found that nutrients released from the bottom sediments contributed a major source of nutrients that was comparable with external loading. Increasing water temperature in 2090 caused stronger summer stratification and higher concentrations of TP and TN from January to April in particular. Following the release from bottom sediments, nutrients (i.e., NH_4–N and PO_4–P, which are readily assimilated by phytoplankton; Burger et al., 2008), accumulate in bottom waters and accelerate phytoplankton growth when subsequently mixed through the water column (Hamilton et al., 2012). Concurrently, increased water temperature directly stimulates growth of phytoplankton, as demonstrated by the result that concentrations of Chl *a* (a proxy for phytoplankton biomass) in lake surface waters were simulated to increase from January to March with increased temperature under a 2090 climate, compared with the baseline climate. Catchment TN loadings (dominated by NO_3–N) decreased by 7.6% while lake surface TN concentrations (dominated by NH_4–N) increased by 44.5% under a 2090 climate, highlighting that careful consideration of the different forms of nitrogen is required to better understand responses to climate change.

Increases in external nutrient loads and increasing temperature in a future climate are likely to act synergistically to negatively impact lake water quality (e.g., Komatsu et al., 2007). Although external nitrogen load from the Puarenga Stream catchment was predicted in this study to decline moderately, by 7.6% with future climate warming of 2090, TN concentrations were much higher for the lake (> 40%), implying that the effects of increased temperatures caused by climate change on phytoplankton physiology, lake stratification and nutrient cycling that are described above can have a major influence on trophic status in this eutrophic polymictic lake.

In addition to overall increased productivity, increased temperatures could lead to increased dominance of cyanobacteria and greater frequency of harmful algal blooms (e.g., Carey et al., 2012), although changes to phytoplankton assemblages were not analysed in this study due to paucity of phytoplankton taxonomy data for validation. Trolle et al. (2011) modelled mean Chl *a* concentrations dominated by chlorophytes and diatoms in a shallow and eutrophic lake (Lake Ellesmere, Canterbury, South Island) using DYRESM–CAEDYM and found that chlorophytes increasingly dominated diatoms with water temperature increases. In eutrophic Lake Rotoehu (maximum depth ~ 13 m) in the Bay of Plenty Region near Lake Rotorua, Trolle et al. (2011) found that under a warmer climate, cyanophytes increased substantially in summer months and diatoms increased in winter months. Lower diatom biomass was also predicted during future warmer climates by Mooij et al. (2007), who examined the impacts of increasing water temperature on a shallow lake in Europe using the PCLake model. These studies indicate that different groups of phytoplankton will respond differently to N and P enrichment, as well as climate change. Variations in internal nutrient loads may also influence the succession of phytoplankton, as noted for Lake Rotorua by Burger et al. (2007b).

The predictions of water quality in lake surface waters with climate change have some degree of uncertainty because future changes in wind speed were not considered in this study. Water column stratification is highly sensitive to this variable (Adrian et al., 2009). Complex temporal and spatial variability in precipitation and temperature projections critically depends on the greenhouse gas forcing among a variety of IPCC models, and represents a source of uncertainty in the predictions of lake water quality since we do not know the precise trajectory of future greenhouse gas emissions (Giorgi, 2010). Furthermore, long–term variability of bottom–sediment composition was not considered in DYRESM–CAEDYM simulations in this study. Rather, fixed sediment release rate parameters were included in the model, with rates adjusted within model simulations according to overlying water temperature and DO. Özkundakci et al. (2012) provide an empirical approach to modify the sediment composition boundary conditions of Lake Rotorua that could be applied in future studies. Nonetheless, these uncertainties are not expected to change the key conclusion that climate change is predicted to lead to an increase in the trophic state of Lake Rotorua, unless more stringent nutrient control measures are adopted.

5. Conclusions

The improved hourly–routing catchment model (SWAT2012 rev629) was combined with the lake model (DYRESM–CAEDYM) to predict the response of polymictic, eutrophic Lake Rotorua to a projected 2090 climate and reductions in nutrient loads from a major sub–catchment (the Puarenga Stream) from wastewater–irrigated forest and farmland. Simulated nutrient loads in the other sub–catchments to the lake were based on current measured loads. The lake model results showed that large reductions to nutrient loads in the Puarenga Stream yielded relatively small improvements in lake water quality. This reflects that, despite being a major sub–catchment, the Puarenga Stream catchment still only contributes ~16% of total nutrient loads to Lake Rotorua. Lake water quality effects caused by direct climate change impacts to in–lake processes were much larger than those caused by indirect climate change impacts to the catchment processes. Further, the overall adverse effects of projected climate change on lake water quality were large and outweighed the effects of nutrient load reductions in one sub–catchment. This finding reflected that Lake Rotorua is polymictic with large nutrient stores in benthic sediments. Consequently, projected increased water temperatures in 2090 will cause more extended periods (i.e., a few weeks) of thermal stratification in summer, which will increase the duration of hypoxic conditions in bottom waters and exacerbate internal nutrient loading. In the short term (i.e., months to a few years) such changes to internal lake nutrient dynamics (i.e., sediment–water exchanges), in conjunction with increased phytoplankton growth rates caused by warmer temperatures, would affect water quality considerably more than changes to external nutrient loading from the catchment. Thus, climate change is expected to confound actions to improve water quality by managing external nutrient loads.

Acknowledgements

This research was supported through the Bay of Plenty Regional Council grant for a Chair in Lake Restoration and Management at the University of Waikato. Further assistance was provided by the New Zealand Ministry of Business, Innovation and Employment (UOWX1503; Enhancing the health and resilience of New Zealand lakes) and the Rotorua Lakes Council. We thank the following people for assistance with data collection: Alison Lowe and Kim Lockie from Rotorua Lakes Council, Andy Bruere and Penny MacCormick from the Bay of Plenty Regional Council, and Cheryl Hindle from Timberlands Limited. We particularly thank Dr. Chonghua Yin, Dr. Yinpeng Li, and Dr. Meng Wang from CLIMsystems for assistance with future climate projections using the SimCLIM software.

Appendix 1. Appendix 1

Statistics used to evaluate model performance. Note: o_n is the n^{th} observed datum, s_n is the n^{th} simulated datum, $\bar{o}$ is the observed mean value, $\bar{s}$ is the simulated daily mean value, and N is the total number of observed data.

Statistic	Definition	Features
Pearson product moment correlation coefficient	$r = \frac{\sum_{n=1}^{N}[(o_n - \bar{o})(s_n - \bar{s})]}{\sqrt{\sum_{n=1}^{N}(o_n - \bar{o})^2 \times \sum_{n=1}^{N}(s_n - \bar{s})^2}}$	Range from −1 to 1. A value of 0 indicates no linear relationship and 1 or -1 indicates a perfect positive or negative linear relationship. Significance of relationship commonly judged by p value (< 0.05; Bewick et al., 2003).
Root mean square error	$\mathrm{RMSE} = \sqrt{\frac{\sum_{n=1}^{N}(s_n - o_n)^2}{N}}$	A value of 0 indicates a perfect fit. This measure is disproportionately affected by large errors.
Mean absolute error	$\mathrm{MAE} = \frac{\sum_{n=1}^{N}\lvert s_n - o_n\rvert}{N}$	A value of 0 indicates a perfect fit. A measure of the mean of the model error.
Percent bias	$\mathrm{PBIAS\%} = \frac{\sum_{n=1}^{N}(o_n - s_n)}{\sum_{n=1}^{N} o_n} \times 100\%$	A value of 0 indicates a perfect fit. Positive values indicate model underestimates and negative values indicate model overestimates.

Appendix 2. Appendix 2

The 22 general circulation models (GCMs) used in this study and the country where each GCM originated. See IPCC (2013).

No.	GCM	Country	No.	GCM	Country
1	ACCESS1–0	Australia	12	HADCM3	UK
2	ACCESS1–3	Australia	13	HADGEM2–CC	UK
3	CANESM2	Canada	14	HADGEM2–ES	UK
4	CSIRO–MK3–6–0	Australia	15	INMCM4	Russia
5	GFDL–CM3	USA	16	IPSL–CM5A–LR	France
6	GFDL–ESM2G	USA	17	IPSL–CM5A–MR	France
7	GFDL–ESM2M	USA	18	IPSL–CM5B–LR	France
8	GISS–E2–H	USA	19	MIROC–ESM	Japan
9	GISS–E2–H–CC	USA	20	MIROC–ESM–CHEM	Japan
10	GISS–E2–R	USA	21	MIROC5	Japan
11	GISS–E2–R–CC	USA	22	MRI–CGCM3	Japan

Appendix 3. Appendix 3

Optimised parameter values with input file extensions for the whole Puarenga Stream catchment for discharge (Q), suspended sediment (SS), total phosphorus (TP), and total nitrogen (TN) concentration simulations. The asterisked values were adjusted beyond the SWAT default range (see text). Input file extensions are shown for each parameter. Parameters are unitless unless otherwise specified. “revap” indicates water movement into the overlying unsaturated layers.

Parameter	Definition	Unit	Default range	Optimal value
Q				
EVRCH.bsn	Reach evaporation adjustment factor		0.5–1	0.7
CH_K2.rte	Effective hydraulic conductivity in the main channel alluvium	mm h^{-1}	0–500	20
CH_N2.rte	Manning's n value for the main channel		0–0.3	0.01
CH_K1.sub	Effective hydraulic conductivity in the tributary channel alluvium	mm h^{-1}	0–300	62
CH_N1.sub	Manning's n value for the tributary channel		0.01–30	12.5
ALPHA_BF.gw	Base flow alpha factor (0–1)		0–1	0.01
GW_DELAY.gw	Groundwater delay	d	0–500	1825*
GW_REVAP.gw	Groundwater “revap” coefficient		0.02–0.2	0.07
GW_SPYLD.gw	Special yield of the shallow aquifer	m^3 m^{-3}	0–0.4	0.2
GWHT.gw	Initial groundwater height	m	0–25	12
GWQMN.gw	Threshold depth of water in the shallow aquifer required for return flow to occur	mm	0–5000	400
RCHRG_DP.gw	Deep aquifer percolation fraction		0–1	0.1
REVAPMN.gw	Threshold depth of water in the shallow aquifer required for “revap” to occur	mm	0–500	344
CANMX.hru	Maximum canopy storage	mm	0–100	0.6
EPCO.hru	Plant uptake compensation factor		0–1	0.34

ESCO.hru	Soil evaporation compensation factor		0–1	0.5
HRU_SLP.hru	Average slope steepness	m m^{-1}	0–0.6	0.1
LAT_TTIME.hru	Lateral flow travel time	d	0–180	3
RSDIN.hru	Initial residue cover	kg ha^{-1}	0–10000	1

	Definition	Unit	Default range	Optimal value
SS				
SLSOIL.hru	Slope length for lateral subsurface flow	m	0–150	15
CH_COV1.rte	Channel erodibility factor		0–0.6	0.1
CH_COV2.rte	Channel cover factor		0–1	0.1
LAT_SED.hru	Sediment concentration in lateral flow and groundwater flow	mg L^{-1}	0–5000	5
OV_N.hru	Manning's n value for overland flow		0.01–30	20
SLSUBBSN.hru	Average slope length	m	10–150	83
SURLAG.bsn	Surface runoff lag coefficient		0.05–24	1
SPCON.bsn	Linear parameter for calculating the maximum amount of sediment that can be re-entrained during channel sediment routing		0.0001–0.01	0.003
SPEXP.bsn	Exponent parameter for calculating sediment re-entrained in channel sediment routing		1–2	1.8
TP				
P_UPDIS.bsn	Phosphorus uptake distribution parameter		0–100	0.5
PHOSKD.bsn	Phosphorus soil partitioning coefficient	m^3 t^{-1}	100–500	100
PPERCO.bsn	Phosphorus percolation coefficient	m^3 t^{-1}	0.01–0.0175	0.005*
PSP.bsn	Phosphorus availability index		0.01–0.7	0.6
GWSOLP.gw	Soluble phosphorus concentration in groundwater loading	mg P L^{-1}	0–1000	0.03
LAT_ORGP.gw	Organic phosphorus in the base flow	mg P L^{-1}	0–200	5
ERORGP.hru	Organic phosphorus enrichment ratio		0–5	0.1
CH_OPCO.rte	Organic phosphorus concentration in the channel	mg P L^{-1}	0–100	0.066
BC4.swq	Rate constant for mineralisation of organic phosphorus to dissolved phosphorus in the reach at 20 °C	d^{-1}	0.01–0.7	0.3
RS2.swq	Benthic (sediment) source rate for dissolved phosphorus in the reach at 20 °C	mg m^{-2} d^{-1}	0.001–0.1	0.02
RS5.swq	Organic phosphorus settling rate in the reach at 20 °C	d^{-1}	0.001–0.1	0.05
USLE_P.mgt	Universal Soil Loss Equation (USLE) support practice factor		0–1	0.5

Parameter	Definition	Unit	Default range	Optimal value
TN				
RSDCO.bsn	Residue decomposition coefficient		0.02–0.1	0.1
CDN.bsn	Denitrification exponential rate coefficient		0–3	0.09
CMN.bsn	Rate factor for humus mineralisation of active organic nitrogen		0.001–0.003	0.001
N_UPDIS.bsn	Nitrogen uptake distribution parameter		0–100	0.5
NPERCO.bsn	Nitrogen percolation coefficient		0–1	0.05
RCN.bsn	Concentration of nitrogen in rainfall	mg N L^{-1}	0–15	0.34
SDNCO.bsn	Denitrification threshold water content		0–1	0.05
HLIFE_NGW.gw	Half–life of nitrate–nitrogen in the shallow aquifer	d	0–200	200
LAT_ORGN.gw	Organic nitrogen in the base flow	mg N L^{-1}	0–200	25
SHALLST_N.gw	Nitrate–nitrogen concentration in the shallow aquifer	mg N L^{-1}	0–1000	1
ERORGN.hru	Organic nitrogen enrichment ratio		0–5	0.1
CH_ONCO.rte	Organic nitrogen concentration in the channel	mg N L^{-1}	0–100	0.34
BC1.swq	Rate constant for biological oxidation of ammonium–nitrogen to nitrite–nitrogen in the reach at 20 °C	d^{-1}	0.1–1	0.55
BC2.swq	Rate constant for biological oxidation of nitrite–nitrogen to nitrate–nitrogen in the reach at 20 °C	d^{-1}	0.2–2	1.1
BC3.swq	Rate constant for hydrolysis of organic nitrogen to ammonium–nitrogen in the reach at 20 °C	d^{-1}	0.2–0.4	0.21
RS3.swq	Benthic (sediment) source rate for ammonium–nitrogen in the reach at 20 °C	mg m^{-2} d^{-1}	0–1	50*
RS4.swq	Rate coefficient for organic nitrogen settling in the reach at 20 °C	d^{-1}	0.001–0.1	0.05

References

Abell, J.M., Hamilton, D.P., Paterson, J., 2011. Reducing the external environmental costs of pastoral farming in New Zealand: experiences from the Te Arawa lakes, Rotorua. Australas. J. Environ. Manag. 18, 139–154.

Abell, J.M., Hamilton, D.P., Rutherford, J.C., 2013. Quantifying temporal and spatial variations in sediment, nitrogen and phosphorus transport in stream inflows to a large eutrophic lake. Environ. Sci. Processes Impacts 15, 1137–1152.

Abell, J.M., McBride, C.M., Hamilton, D.P., 2015. Lake Rotorua Wastewater Discharge: Environmental Effects Study, ERI Report No. 80, Client Report Prepared for Rotorua Lakes Council, Environmental Research Institute. Faculty of Science and Engineering, the University of Waikato, Hamilton, New Zealand, pp. 122.

Adrian, R., O'Reilly, C.M., Zagarese, H., Baines, S.B., Hessen, D.O., Keller, W., Livingstone,

D.M., Sommaruga, R., Straile, D., Van Donk, E., Weyhenmeyer, G.A., Winder, M., 2009. Lakes as sentinels of climate change. Limnol. Oceanogr. 54, 2283–2297.
Allan, M.G., Hamilton, D.P., Hicks, B.J., Brabyn, L., 2011. Landsat remote sensing of chlorophyll a concentrations in central North Island lakes of New Zealand. Int. J. Rem. Sens. 32, 2037–2055.
Anastasiadis, S., Nauleau, M.-L., Kerr, S., Cox, T., Rutherford, K., 2011. Water Quality Management in Lake Rotorua: a Comparison of Regulatory Approaches Using the NManager Model. In: Proceedings of the 52nd Annual Conference of the New Zealand Association of Economists, Wellington, New Zealand, pp. 46.
Arheimer, B., Dahné, J., Donnelly, C., 2012. Climate change impact on riverine nutrient load and land-based remedial measures of the Baltic Sea Action Plan. Ambio 41, 600–612.
Arnell, N.W., Halliday, S.J., Battarbee, R.W., Skeffington, R.A., Wade, A.J., 2015. The implications of climate change for the water environment in England. Prog. Phys. Geogr. 39, 93–120.
Arnold, J., Kiniry, J., Srinivasan, R., Williams, J., Haney, E., Neitsch, S., 2013. Soil & Water Assessment Tool Input/output Documentation Version 2012, Technical Report No 439. Texas Water Resources Institute, College Station, TX, the United States, pp. 651.
Bain, D.J., Green, M.B., Campbell, J.L., Chamblee, J.F., Chaoka, S., Fraterrigo, J.M., Kaushal, S.S., Martin, S.L., Jordan, T.E., Parolari, A.J., 2012. Legacy effects in material flux: structural catchment changes predate long–term studies. Bioscience 62, 575–584.
Beets, P.N., Gielen, G., Oliver, G.R., Pearce, S.H., Graham, J.D., 2013. Determination of the Level of Soil N and P Storage and Soil Health at the Rotorua Land Treatment Site, Scion Report 50659. New Zealand Forest Research Institute Limited, Rotorua, New Zealand, pp. 39.
Bewick, V., Cheek, L., Ball, J., 2003. Statistics review 7: correlation and regression. Crit. Care 7, 451–459.
Bruce, L.C., Hamilton, D.P., Imberger, J., Gal, G., Gophen, M., Zohary, T., Hambright, K.D., 2006. A numerical simulation of the role of zooplankton in C, N and P cycling in Lake Kinneret, Israel. Ecol. Model. 193, 412–436.
Burger, D.F., Hamilton, D.P., Pilditch, C.A., Gibbs, M.M., 2007a. Benthic nutrient fluxes in a eutrophic, polymictic lake. Hydrobiologia 584, 13–25.
Burger, D.F., Hamilton, D.P., Hall, J.A., Ryan, E.F., 2007b. Phytoplankton nutrient limitation in a polymictic eutrophic lake: community versus species–specific responses. Fund. Appl. Limnol. 169, 57–68.
Burger, D.F., Hamilton, D.P., Pilditch, C.A., 2008. Modelling the relative importance of internal and external nutrient loads on water column nutrient concentrations and phytoplankton biomass in a shallow polymictic lake. Ecol. Model. 21, 411–423.
Burns, N.M., Rutherford, J.C., Clayton, J.S., 1999. A monitoring and classification system for New Zealand lakes and reservoirs, Lake Reserv. Manage 15, 255–271.
Cao, W., Bowden, W.B., Davie, T., Fenemor, A., 2006. Multi–variable and multi–site calibration and validation of SWAT in a large mountainous catchment with high spatial variability. Hydrol. Process. 20, 1057–1073.
Carey, C.C., Ibelings, B.W., Hoffman, E.P., Hamilton, D.P., Brookes, J.D., 2012. Eco-physiological adaptations that favour freshwater cyanobacteria in a changing climate. Water Res. 46, 1394–1407.
Cartwright, I., Gilfedder, B., Hofmann, H., 2014. Contrasts between estimates of baseflow help discern multiple sources of water contributing to rivers. Hydrol. Earth Syst. Sci. 18, 15–30.
Copetti, D., Tartari, G., Morabito, G., Oggioni, A., Legnani, E., Imberger, J., 2006. A biogeochemical model of Lake Pusiano (North Italy) and its use in the predictability of phytoplankton blooms: first preliminary results. J. Limnol. 65, 59–64.
Debele, B., Srinivasan, R., Parlange, J.Y., 2008. Coupling upland watershed and downstream water body hydrodynamic and water quality models (SWAT and CE-QUAL-W2) for better water resources management in complex river basins. Environ. Model. Assess. 13, 135–153.
Donnelly, C., Strömqvist, J., Arheimer, B., 2011. Modelling climate change effects on nutrient discharges from the baltic sea catchment, in: water quality: current trends and expected climate change impacts. In: Proceedings of Symposium H04 Held During IUGG2011, Melbourne Australia 348. IAHS Publ., pp. 145–150.
Environment Bay of Plenty, 1997. Rotorua Lakes Summary Report, Environmental Report 97/21, Whakatāne, New Zealand. pp. 48.
Environment Bay of Plenty, 2007. Historical Data Summary, Environmental Publication 07/06–1, Whakatāne, New Zealand. pp. 522.
Environment Bay of Plenty, 2010. Soils of the Bay of Plenty Volume 1: Western Bay of Plenty, Environmental Publication 2010/11–1, Whakatāne, New Zealand. pp. 182.
Fertiliser and Lime Research Centre, 2014. Sustainable Nutrient Management in New Zealand Agriculture: Introductory Notes and Mastery Test, Institute of Agriculture & Environment. Massey University, Palmerston North, New Zealand, pp. 94.
Foote, K.J., Joy, M.K., Death, R.G., 2015. New Zealand dairy farming: milking our environment for all its worth. Environ. Manag. 56, 709–720.
Gabriele, W., Welti, N., Hein, T., 2013. Limitations of stream restoration for nitrogen retention in agricultural headwater streams. Ecol. Eng. 60, 224–234.
Giorgi, F., 2010. Uncertainties in climate change projections, from the global to the regional scale. EPJ Web Conf. 9, 115–129.
Glavan, M., Ceglar, A., Pintar, M., 2015. Assessing the impacts of climate change on water quantity and quality modelling in small Slovenian Mediterranean catchment – lesson for policy and decision makers. Hydrol. Process. 29, 3124–3144.
Guzman, J.A., Moriasi, D.N., Gowda, P.H., Steiner, J.L., Starks, P.J., Arnold, J.G., Srinivasan, R., 2015. A model integration framework for linking SWAT and MODFLOW. Environ. Model. Software 73, 103–116.
Hamilton, D.P., Alexander, W., Burger, D., 2004. Nutrient Budget for Lakes Rotoiti and Rotorua Part 1: Internal Nutrient Loads. Centre for Biodiversity and Ecology Research, the University of Waikato, Hamilton, New Zealand, pp. 49.
Hamilton, D.P., McBride, C.G., Jones, H.F.E., 2015. Assessing the Effects of Alum Dosing of Two Inflows to Lake Rotorua against External Nutrient Load Reductions: Model Simulations for 2001-2012, Report 49, Environmental Research Institute. University of Waikato, Hamilton, New Zealand, pp. 56.
Hamilton, D.P., Özkundakci, D., McBride, C.G., Ye, W., Luo, L., Silvester, W., White, P., 2012. Predicting the Effects of Nutrient Loads, Management Regimes and Climate Change on Water Quality of Lake Rotorua. University of Waikato Report 005, Environmental Research Institute, University of Waikato, Hamilton, New Zealand, pp. 73.
Hamilton, D.P., Schladow, S.G., 1997. Prediction of water quality in lakes and reservoirs. Part I – model description. Ecol. Model. 96, 91–110.
Hamilton, D.P., Salmaso, N., Paerl, H.W., 2016. Mitigating harmful cyanobacterial blooms: strategies for control of nitrogen and phosphorus loads. Aquat. Ecol. 50, 351–366.
Herger, N., Sanderson, B.M., Knutti, R., 2015. Improved pattern scaling approaches for the use in climate impact studies. Geophys. Res. Lett. 42, 3486–3494.
Hien, H.N., Hoang, B.H., Huong, T.T., Than, T.T., Ha, P.T.T., Toan, T.D., Son, N.M., 2016. Study of the climate change impacts on water quality in the upstream portion of the Cau River Basin, Vietnam. Environ. Model. Assess. 21, 261–277.
Hoare, R.A., 1980. Inflows to lake rotorua. J. Hydrol. 19, 49–59.
Huntingford, C., Booth, B., Sitch, S., Gedney, N., Lowe, J., Liddicoat, S., Mercado, L., Best, M., Weedon, G., Fisher, R.A., Good, P., Zelazowski, P., Spessa, A.C., Jones, D.C., 2010. IMOGEN: an intermediate complexity model to evaluate terrestrial impacts of a changing climate. Geosci. Model Dev. (GMD) 3, 679–687.
Hussain, I., Raschid, L., Hanjra, M.A., Marikar, F., van der Hoek, W., 2002. Wastewater Use in Agriculture: Review of Impacts and Methodological Issues in Valuing Impacts. Working Paper 37, International Water Management Institute, Colombo, Sri Lanka, pp. 62.
IPCC, 2013. Climate Change 2013: the physical science basis. In: Stocker, T.F., Qin, D., Plattner, G.-K., Tignor, M.M.B., Allen, S.K., Boschung, J., Nauels, A., Xia, Y., Bex, V., Midgley, P.M. (Eds.), Contribution of Working Group I to the Fifth Assessment Report of the Intergovernmental Panel on Climate Change. Cambridge University Press, Cambridge, New York, the United States, pp. 1535.
Jeppesen, E., Kronvang, B., Meerhoff, M., Søndergaard, M., Hansen, K.M., Andersen, H.E., Lauridsen, T.L., Beklioglu, M., Ozen, A., Olesen, J.E., 2009. Climate change effects on runoff, catchment phosphorus loading and lake ecological state, and potential adaptations. J. Environ. Qual. 38, 1930–1941.
Komatsu, E., Fukushima, T., Harasawa, H., 2007. A modeling approach to forecast the effect of long–termclimate change on lake water quality. Ecol. Model. 209, 351–366.
Kourzeneva, E., Martin, E., Batrak, Y., Le Moigne, P., 2012. Climate data for parameterisation of lakes in numerical weather prediction models. Tellus 64, 1–17.
Krebs, C.J., 2008. Restoration ecology applies ecological knowledge to repair damaged communities. In: Krebs, C.J. (Ed.), The Ecological World View. University of California Press, Berkeley and Los Angeles, California, the United States, pp. 300.
Kurylyk, B.L., Bourque, C.P.-A., MacQuarrie, K.T.B., 2013. Potential surface temperature and shallow groundwater temperature response to climate change: an example from a small forested catchment in east–central New Brunswick (Canada), Hydrol. Earth Syst. Sc. 17, 2701–2716.
Lopez, A., Suckling, E.B., Smith, L.A., 2014. Robustness of pattern scaled climate change scenarios for adaptation decision support. Climatic Change 122, 555–566.
Losordo, T.M., Piedrahita, R.H., 1991. Modelling temperature variation and thermal stratification in shallow aquaculture ponds. Ecol. Model. 54, 189–226.
Lowe, A., Gielen, G., Bainbridge, A., Jones, K., 2007. The rotorua land treatment systems after 16 years. In: New Zealand land treatment collective, Proceedings for the 2007 Annual Conference, 14–16 March 2007, Rotorua, New Zealand, pp. 66–73.
Lustenberger, A., Knutti, R., Fischer, E.M., 2014. The potential of pattern scaling for projecting temperature-related extreme indices. Int. J. Climatol. 34, 18–26.
McGhee, R.F., 1983. Experiences in developing a chlorophyll *a* standard in the Southeast to protect lakes, reservoirs and estuaries. In: Lake Restoration Protection and Management, Proc. 2nd Annu. Conf., N. Am. Lake Manage. Soc., EPA 440/5–83–001. U.S. Environ. Prot. Agency, Washington, D.C, pp. 163–165.
Me, W., Abell, J.M., Hamilton, D.P., 2015. Effects of hydrologic conditions on SWAT model performance and parameter sensitivity for a small, mixed land use catchment in New Zealand, Hydrol. Earth Syst. Sc. 19, 4127–4147.
Me, W., Hamilton, D.P., Abell, J.M., 2017. Simulating Discharge and Contaminant Loads from the Waipa Stream Catchment under Different Irrigation Scenarios Using the SWAT Model, Client Report Prepared for Rotorua Lakes Council, ERI Report No. 98. Faculty of Science and Engineering, University of Waikato, Hamilton, New Zealand, pp. 32.
Me, W., 2017. Modelling Temporal Dynamics of Discharge and Nutrient Loading from a Mixed Land Use Catchment, and Interactions with a Eutrophic, Temperate Lake under Climate Change. Doctor of Philosophy (PhD) thesis. Biological Sciences, the University of Waikato, Hamilton, New Zealand, pp. 196.
Mitchell, T.D., 2003. Pattern scaling: an examination of the accuracy of the technique for describing future climates. Climatic Change 60, 217–242.
Mooij, W.M., Janse, J.H., De Senerpont Domis, L.N., Hülsmann, S., Ibelings, B.W., 2007. Predicting the effect of climate change on temperate shallow lakes with the ecosystem model PCLake. Hydrobiologia 584, 443–454.
Morcom, C.P., 2013. Nitrogen Yields into the Tauranga Harbour Based on Sub–catchment Land Use. Master thesis. Master of Science, the University of Waikato, Hamilton, New Zealand, pp. 132.
Morgenstern, U., Daughney, C., Leonard, G., Gordon, D., Donath, F., Reeves, R., 2015. Using groundwater age and hydrochemistry to understand sources and dynamics of nutrient contamination through the catchment into Lake Rotoroa, New Zealand. Hydrol. Earth Syst. Sci. 19, 803–822.
Moriasi, D.N., Arnold, J.G., Van Liew, M.W., Bingner, R.L., Harmel, R.D., Veith, T.L.,

2007. Model evaluation guidelines for systematic quantification of accuracy in watershed simulations. T. ASAE 50, 885–900.
Morris, M.D., 1991. Factorial sampling plans for preliminary computational experiments. Technometrics 33, 161–174.
Mueller, H., Hamilton, D.P., Doole, G.J., 2015. Response lags and environmental dynamics of restoration efforts for Lake Rotorua, New Zealand. Environ. Res. Lett. 10.
Murphy, J.M., Booth, B.B.B., Collins, M., Harris, G.R., Sexton, D.M.H., Webb, M.J., 2007. A methodology for probabilistic predictions of regional climate change from perturbed physics ensembles. Phil. Trans. R. Soc. A. 365, 1993–2028.
Narasimhan, B., Srinivasan, R., Bednarz, S.T., Ernst, M.R., Allen, P.M., 2010. A comprehensive modeling approach for reservoir water quality assessment and management due to point and nonpoint source pollution. T. ASABE. 53, 1605–1617.
Neitsch, S.L., Arnold, J.G., Kiniry, J.R., Williams, J.R., 2011. Soil and Water Assessment Tool Theoretical Documentation Version 2009, Texas Water Resources Institute Technical Report No. 406. Texas A&M University System, College Station, Texas, pp. 647.
OECD (Organisation for Economic Co–operation and Development), 2001. Environmental Performance Reviews: Germany, Environmental Performance, Paris, France. pp. 236.
Özkundakci, D., McBride, C.G., Hamilton, D.P., 2012. Parameterisation of sediment geochemistry for simulating water quality responses to long-term catchment and climate Changes in Polymictic, eutrophic Lake Rotorua, New Zealand. Water Pol. XI, 171–182.
Robertson, D.M., Saad, D.A., Christiansen, D.E., Lorenz, D.J., 2016. Simulated impacts of climate change on phosphorus loading to Lake Michigan. J. Great Lake. Res. 42, 536–548.
Rutherford, J.C., Dumnov, S.M., Ross, A.H., 1996. Predictions of phosphorus in lake rotorua following load reductions. New Zeal. J. Mar. Fresh. 30, 383–396.
Rutherford, J.C., Palliser, C., Wadhwa, S., 2009. Nitrogen Exports from the Lake Rotorua Catchment – Calibration of the ROTAN Model, NIWA Client Report: HAM2009-019. National Institute of Water & Atmospheric Research Ltd, Hamilton, New Zealand, pp. 66.
Santer, B.D., Wigley, T.M.L., Schlesinger, M.E., Mitchell, J.F.B., 1990. Developing Climate Scenarios from Equilibrium GCM Results, Report No. 47, Max–Planck–Institute, Fuer Meteorologie. Germany, Hamburg, pp. 31.
Saunders, W.M.H., 1965. Phosphate retention by New Zealand soils and its relationship to free sesquioxides, organic matter, and other soil properties. NZJAR (N. Z. J. Agric. Res.) 8, 30–57.
Scholes, P., 2011. 2010/2011 Rotorua Lakes Trophic Level Index Update. Bay of Plenty Regional Council Environmental Publication 2011/17, Whakatane, New Zealand, pp. 37.
Scavia, D., Allan, J.D., Arend, K.K., Bartell, S., Beletsky, D., Bosch, N.S., Brandt, S.B., Briland, R.D., Daloğlu, I., DePinto, J.V., Dolan, D.M., Evans, M.A., Farmer, T.M., Goto, D., Han, H., Höök, T.O., Knight, R., Ludsin, S.A., Mason, D., Michalak, A.M., Richards, R.P., Roberts, J.J., Rucinski, D.K., Rutherford, E., Schwab, D.J., Sesterhenn, T.M., Zhang, H., Zhou, Y., 2014. Assessing and addressing the re-eutrophication of Lake Erie: central basin hypoxia. J. Great Lake. Res. 40, 226–246.
Sharpley, A., Jarvie, H.P., Buda, A., May, L., Spears, B., Kleinman, P., 2014. Phosphorus legacy: overcoming the effects of past management practices to mitigate future water quality impairment. J. Environ. Qual. 42, 1308–1326.
Smith, V.H., Wood, S.A., McBride, C.G., Atalah, J., Hamilton, D.P., Abell, J., 2016. Phosphorus and nitrogen loading restraints are essential for successful eutrophication control of Lake Rotorua, New Zealand. Inland Waters 6, 273–283.
Spears, B.M., Dudley, B., Reitzel, K., Rydin, E., 2013. Geo-engineering in lakes-a call for consensus. Environ. Sci. Technol. 47, 3953–3954.
Stuber, R.J., Gebhart, G., Maughan, O.E., 1982. Habitat Suitability Index Models: Largemouth Bass, FWS/OBS–82/10.16. Fish Wildl. Serv., U.S. Dept. Int., Washington, D.C., pp. 32.
Tebaldi, C., Arblaster, J.M., 2014. Pattern-scaling: its strengths and limitations, and an update on the latest model simulations. Climatic Change 122, 459–471.
Todd, M.C., Taylor, R.G., Osborn, T.J., Kingston, D.G., Arnell, N.W., Gosling, S.N., 2011. Uncertainty in climate change impacts on basin-scale freshwater resources - preface to the special issue: the QUEST-GSI methodology and synthesis of results, Hydrol. Earth Syst. Sc. 15, 1035–1046.
Touma, D., Ashfaq, M., Nayak, M.A., Kao, S.C., Diffenbaugh, N.S., 2015. A multi-model and multi-index evaluation of drought characteristics in the 21st century. J. Hydrol. 526, 196–207.
Trolle, D., Skovgaard, H., Jeppesen, E., 2008. The Water Framework Directive: setting the phosphorus loading target for a deep lake in Denmark using the 1D lake ecosystem model DYRESMeCAEDYM. Ecol. Model. 219, 138–152.
Trolle, D., Hamilton, D.P., Pilditch, C.A., Duggan, I.C., Jeppesen, E., 2011. Predicting the effects of climate change on trophic state of three morphologically varying lakes: implications for lake restoration and management. Environ. Model. Software 26, 354–370.
Van Vuuren, D.P., Edmonds, J., Kainuma, M.L.T., Riahi, K., Thomson, A., Matsui, T., Hurtt, G., Lamarque, J.-F., Meinshausen, M., Smith, S., Grainer, C., Rose, S., Hibbard, K.A., Nakicenovic, N., Krey, V., Kram, T., 2011. The representative concentration pathways: an overview. Climatic Change 109, 5–31.
Ward, A.S., Gooseff, M.N., Fitzgerald, M., Voltz, T.J., Binley, A.M., Singha, K., 2012. Hydrologic and geomorphic controls on hyporheic exchange during base flow recession in a headwater mountain stream. Water Resour. Res. 48 W04513.
Wilhelm, S., Adrian, R., 2008. Impact of summer warming on the thermal characteristics of a polymictic lake and consequences for oxygen, nutrients and phytoplankton. Freshw. Biol. 53, 226–237.
Yin, C., Li, Y., Urich, P., 2013. SimCLIM2013 Data Manual. CLIMsystems, Hamilton, New Zealand, pp. 35.
Zhang, D., Chen, X., Yao, H., Lin, B., 2015. Improved calibration scheme of SWAT by separating wet and dry seasons. Ecol. Model. 301, 54–61.
Zogg, G.P., Zak, D.R., Pregitzer, K.S., Burton, A.J., 2000. Microbial immobilization and the retention of anthropogenic nitrate in a northern hardwood forest. Ecology 81, 1858–1866.